


Lunar meteorites from northern Africa

Randy L. KOROTEV ^{1*}, and Anthony J. IRVING²

¹Department of Earth and Planetary Sciences and McDonnell Center for the Space Sciences, Washington University, Saint Louis, Missouri 63130, USA

²Department of Earth and Space Sciences, University of Washington, Seattle, Washington 98195, USA

*Corresponding author: E-mail: korotev@wustl.edu

(Received 13 November 2019; revision accepted 22 November 2020)

Abstract—We report bulk composition data for 235 stones of ~77 lunar meteorites from northern Africa and 33 lunar meteorites from elsewhere. About 27% of the African meteorites are typical feldspathic lunar rocks, all breccias of similar bulk composition, for example, 3–5% FeO and low concentrations of incompatible elements. Nevertheless, these meteorites have a large range in Mg' (whole-rock mole% $Mg/[Mg + Fe]$), 57–77 (mean: 65.5), and this parameter does not correlate with either albite content of the plagioclase or concentrations of incompatible elements. From this observation, we conclude that feldspathic lunar meteorites do not support the hypotheses that the anorthositic, precursor plutonic rocks of the meteorite breccias all crystallized from a common magma. Among feldspathic lunar meteorites, Mg' increases with normative olivine abundance but is uncorrelated with normative pyroxene abundance, that is, high- Mg' feldspathic rocks of the early lunar crust were troctolitic, not noritic. The NWA 5744 (Northwest Africa) clan of lunar meteorites are anorthositic troctolites (59–75% plagioclase, 15–26% olivine, Fe_{77-80}) with very low concentrations of incompatible elements ($2.6 \times CI$) compared to troctolites in the Apollo collection. They may represent the lower feldspathic crust or differentiated impact melt from portions of the highlands distant from the PKT (Procellarum KREEP Terrane). About 31% of the lunar meteorites from northern Africa, all breccias, are, by lunar standards, moderately mafic (5–13% FeO) but more magnesian than mixtures of typical feldspathic meteorite and mare basalt, implying that they represent moderately mafic regions of the highlands or originate from the South Pole–Aitken basin. With $\sim 6 \mu g g^{-1}$ Th, two NWA meteorites likely originate from the PKT. Including the unique NWA 773 clan, at least six of the northern Africa meteorites are, or are dominated by, unbrecciated basalts and gabbros of mare affinity. We estimate that the ~341 lunar meteorite stones (Africa and elsewhere) for which there are data represent 131–147 terrestrially unpaired meteorites and 109–134 lunar launch sites.

INTRODUCTION

The first lunar meteorite from northern Africa to be recognized was DaG (Dar al Gani) 262, a 513 g stone found in Libya on March 23, 1997 (Bischoff and Weber 1997; Bischoff et al. 1998; Fig. 1). This discovery came 17 years after the first lunar meteorite was found in Antarctica (Yamato 791197, November 20, 1979, but not recognized as lunar until 1984 [Yanai and Kojima 1984]). As of December 31, 2019, 22.8 years later, there are 281 named lunar meteorite stones from northern Africa (Table 1). This value is

71% of all lunar meteorites ($N = 398$) and $1.5 \times$ the number of Martian meteorite stones from northern Africa (Table 1 and online Meteoritical Bulletin Database, hereafter “MetBull”; Grossman 2020). The combined mass is 491.8 kg, a value that is 93.8% of all lunar meteorites and equivalent to $1.85 \times$ the mass of rocks in the Apollo collection (i.e., samples >1 cm in size; table 3.2 of Vaniman et al. 1991). On average, lunar meteorite stones from northern Africa tend to be ~30 times larger than those from Antarctica and Oman and three times larger than Martian meteorites from northern Africa (Table 1). None of the lunar meteorite

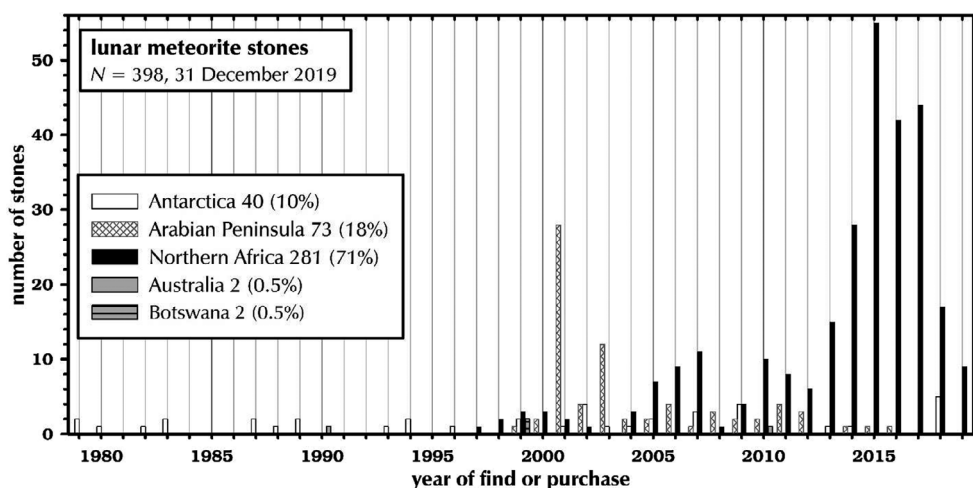


Fig. 1. Histogram of the number of lunar meteorite stones as a function of year of find (if known) or purchase (data from Grossman 2020). All Arabian Peninsula stones are from Oman except for two that are from Saudi Arabia. For northern Africa, find dates to at least the year and month are reported for only 18% of the stones. The height of the bars representing the last ~5 years will increase with time. Of the northern Africa stones for which the find or purchase year and month are known ($N = 281$), 40% have names approved within 0.5 years, 48% within 0.5–2 years, 8% within 2–5 years, and 4% within 5–14 years (Dar al Gani 1058 holds the record at 14 years). This plot is misleading in that it counts named stones, which are known precisely, not meteorites, for which assumptions are required (see Table 4). For example, the spike at 2001 of 28 Oman stones includes 12 named stones of one meteorite and 9 named stones of another.

from Northern Africa or elsewhere has been a witnessed fall.

We have studied a large fraction of the lunar meteorite stones recovered in the barren, sand-free regions of northern Africa by standard petrographic techniques (50%) and determination of bulk chemical composition by INAA (instrumental neutron activation analysis; 74%). Most of the main text of this paper is devoted to comparing the numerous lunar meteorites from northern Africa to each other and those from elsewhere and summarizing what chemical compositions of the meteorites reveal about lunar geology. We also address the issue of pairing, that is, different stones from the same meteoroid that all landed in a small area within seconds to minutes of each other (terrestrial pairing) or different meteoroids ejected by a single impact on the Moon that landed on Earth at different places and times (launch pairing). Most of the justification for our pairing conclusions is presented in the supporting information, but we introduce the issues here. Throughout this work, we use the term “stone” to refer to the entire reported mass, regardless of number of “pieces” (which range from 1 to “many,” Table S1 in supporting information), of a meteorite (MetBull) or assumed pair.

THE PAIRING PROBLEM

Meteorites from northern African countries (Table 1) have been found mainly by nomads and prospectors. Most specimens have become available to

scientists through indirect and poorly documented circumstances that have been driven by commerce, not science. Only 22% of the descriptions of lunar meteorites in the MetBull include information about reported find location that is more specific than, for example, “southern Morocco,” yet 60% include the place of purchase. For only 5% of the meteorites is the find date reported and for only 23 is the find year reported. Nevertheless, the find rate has been increasing up until the last 4 years (Fig. 1).

In northern Africa, stones from terrestrial pair groups, or even fragments from a single rock, have been geographically separated by anthropogenic means and reported find locations are not as accurate nor as reliable as meteoriticists are accustomed for meteorites from other regions. This process is the main reason that the ratio of number of named stones to estimated number of meteorites (below), 2.4, is considerably greater than unity. Thus, we do not rely heavily on reported find or purchase locations to argue for or against pairing. Instead, we mainly use compositional and petrographic similarities and differences to address possible pairing relationships.

Neither bulk composition nor petrography can prove or disprove pairing. Nevertheless, our experience with lunar meteorites from Antarctica and Oman, where find locations are well established, suggests that, more often than not, different stones of a terrestrial pair group are compositionally and texturally similar. As we document here, however, some lunar meteorites are

Table 1. Number (N) and mass data for lunar, Martian, and other stony meteorites.

Place	N stony	N Moon	N Mars	% Moon	% Mars	kg Moon	kg Mars	Mean kg Moon	Mean kg Mars
Northern Africa	13,473	281	191	2.09	0.32	491.795	114.678	1.75	0.60
Algeria	983	16		1.63		7.1		0.44	
Egypt	80	0		0.00		0.0			
Libya	1496	7		0.47		4.7		0.67	
Mali	35	5		14.29		11.8		2.37	
Mauritania	107	12		11.21		39.7		3.31	
Morocco	1424	44		3.09		40.3		0.91	
Morocco?	5	0		0.0		0.0			
Niger	59	1		1.69		0.2		0.15	
Sudan	9	1		11.11		0.3		0.26	
Tunisia	76	0		0.0		0.0			
Western Sahara	210	22		10.48		87.7		3.99	
(Northwest Africa)	8989	173		1.92		300.1		1.73	
(Sahara)	958	0		0.0		0.0			
Antarctica	39,739	40	30	0.10	0.05	5.651	28.829	0.14	0.96
Australia	705	2		0.28		0.056		0.03	
Botswana	11	2		18.18		14.085		7.04	
Oman	3902	71	18	1.82	0.03	11.222	12.938	0.16	0.72
Saudi Arabia	103	2		1.94		1.460		0.73	
Elsewhere	0	0	7	0.0	0.01	0.0	29.	0.00	4.2
All	58,891	398	246	0.68	0.42	524.3	186.	1.32	0.75

Note: Data from the Meteoritical Bulletin Database as of December 31, 2019 (Grossman 2020). The data of the second column represent 93% of all stony meteorites.

compositionally heterogeneous at the scale of our sampling and multiple subsamples of two or more samples or pieces of a given meteorite do not always overlap in composition. Conversely, but more rarely, some meteorites are nearly indistinguishable in composition from each other but have substantially different textures (e.g., NWA 10415 and NWA 11077, see supporting information). Hence, composition and petrography are useful, but not definitive, for establishing pairing. Our suggestions regarding pairing (Table S1) are merely hypotheses that can be tested by petrography more extensive than that of the MetBull classifications or by other techniques, for example, crystallization ages for igneous rocks (e.g., Elardo et al. 2013) or cosmic-ray exposure ages for breccias (e.g., Nishiizumi et al. 2016). It is likely that some of our suggested pairings are launch pairs, not terrestrial pairs. Thus, throughout the paper, we use the term “pair” loosely to refer to both scenarios. Finally, for convenience, we use the term “clan” (e.g., the NWA 4936 clan) to refer to a group of meteorites of similar composition that are likely paired but perhaps are not.

AJI has classified 130 of the 281 lunar meteorites from Northern Africa listed in the MetBull as of December 31, 2019 (Table S1). RLK has chemically analyzed 1492 subsamples of 320 lunar rock samples from northern Africa. Two-thirds of the samples were from donors who had submitted rock samples to AJI for classification or

verification that the rocks were meteorites. Of the samples analyzed by RLK, 70% ($N = 224$) were from type specimens; 7% ($N = 21$) purchased from reputable dealers as named lunar meteorites; and 23% ($N = 75$) were donated by dealers or collectors, many of whom are the holders of record of the main mass of the meteorite as listed in the MetBull. Among the donations, 57% ($N = 43$) were alleged by the donor to be a sample of a named lunar meteorite and, on the basis of our data, we have no reason to doubt any of those claims. Most of the rest, 36% ($N = 27$), were submitted with no allegation that they were meteorites but which we conclude are, in fact, samples of pairs to or pieces of named stones on the basis of compositional similarity to named meteorites that we have studied. In tables and figures, our samples of the latter are designated, for example, “NWA 2995 pair,” with the caveat that the pairing is an assumption based on composition, petrography, and often timing in that we acquired the sample about the same time as we acquired the type specimen. This particular “pairing problem” is somewhat akin to numerous poorly documented iron meteorites that are actually just stones of Campo del Cielo (Wasson 2019).

The remaining 7% of donations ($N = 5$), however, have compositional and petrographic characteristics consistent only with lunar rocks but in detail are unlike any named meteorite that we have studied. They remain unnamed as meteorites for lack of a type specimen. In

the tables and figures, we present data for these rocks and designate them “lunar rock 1,” “lunar rock 2,” etc., with no discussion (Table S1).

SAMPLES AND SAMPLING

As noted above, most of the samples described and analyzed here were submitted to AJI for classification by finders, sellers, or purchasers; nearly all such samples are from the type specimen housed mostly at the Burke Museum, University of Washington, but also elsewhere (notably in the repository of the Planetary Studies Foundation housed at Yale University). Other samples were donated to or purchased by RLK. As commodities for private collections or for scientific studies, lunar meteorites are ephemeral in that the time-window for acquiring a sample of some has been on the order of days to weeks. Details of the sources are presented in Table S2 in supporting information. RLK obtained samples in a variety of states: sawn slices (some polished on one side), fragments of slices, fragments chipped off the rocks, and fragments with fines (Fig. S1 in supporting information). Many of the fragmented samples are from the near surface of the stone before it was sawn, and several of these are visibly weathered.

Sampling procedures are described in Korotev et al. (2009). The pertinent aspects are that the samples are not subjected to any chemical treatment and, except for subdivision, are largely analyzed “as is.” All material greater than 3 mm in maximum dimension was wrapped in glassine weighing paper and fragmented by striking with a stainless steel hammer or hammer and chisel. Typically, for each meteorite stone, 4–10 subsamples of 20–35 mg each were prepared and weighed into ultrapure silica tubes for neutron irradiation and radioassay (Fig. S2 in supporting information). Meteorites for which we have analyzed a large number of subsamples are usually those for which we obtained samples from more than one source or several different pieces at different times, often not knowing whether or not they were samples of the same meteorite prior to analysis. At one extreme, subsamples consisted of only one or two fragmented chips; at the other, subsamples consisted mainly of crumbs and fines generated in the fragmentation procedure. In a very few cases, we analyzed samples of carefully collected, clean wet saw cutting “dust.” The number of subsamples and analyzed mass of each stone is reported in Tables S2 and S3 in supporting information.

CHEMICAL ANALYSIS

This paper relies mainly on compositional data obtained by INAA, which is a bulk or “whole-rock”

technique. INAA procedures are essentially those of Korotev et al. (2009) with two exceptions since 2014, described in the supporting information, that moderately enhanced precision. INAA data for all subsamples ($N = 1809$) are presented in Table S2 and mass-weighted mean concentrations by stone are summarized in Table S3. For some stones, we obtained major element data by EPMA (electron probe microanalysis) of “fused beads” prepared from INAA subsamples after radioassay as described in Korotev et al. (2009). Major element data are presented in Table S4 in supporting information.

Some of the INAA data synthesized here were published in previous papers as mass-weighted means only. These papers are cited in Table S2. We use this opportunity to present our subsample data for some meteorites found elsewhere than northern Africa that we have only published as mass-weighted means in previous papers or graphically in abstracts (Table S2). These meteorites include AaU 012 (Abar al' Uj 012, Saudi Arabia; Mészáros et al. 2016); Calalong Creek (Australia, Korotev et al. 2009); Lynch 002 (Australia, Korotev 2013); Kalahari 008 and 009 (Botswana, Korotev et al. 2009); and several from Antarctica, including DEW (Mount DeWitt) 12007 and MIL (Miller Range) 13317.

RESULTS AND DISCUSSION

Among all lunar meteorites, the vast majority (95%) are breccias; the rest are mafic igneous rocks (basalt, gabbro, diabase). Many modifiers have been applied to the breccias, either textural (e.g., monomict, polymict, regolith, fragmental, clast-rich, glassy matrix, granulitic, impact melt) or mineralogical (anorthositic, feldspathic, mafic, basaltic, troctolitic, KREEP-bearing). We emphasize that, in the MetBull descriptions, there is considerable inconsistency among different petrographers in the application of these terms. For example, the ~40 stones of the NWA 8046 clan have been classified or described (MetBull classifications) as feldspathic breccia, feldspathic fragmental breccia, feldspathic regolith breccia, polymict breccia, highland polymict breccia, polymict feldspathic breccia, and melt breccia while the stones of the NWA 8455 clan are classified as feldspathic breccia, polymict breccia, melt matrix breccia, granulitic troctolitic breccia, and olivine leuco-gabbro. In both cases, the diversity is caused in part by natural heterogeneity of the breccias and classifications being made from small (one to a few cm²) thin sections or polished sample surfaces that are rich in coarse-grained clasts, some >1 cm in size. Some breccias described as “feldspathic” are relatively mafic by lunar standards. For consistency, in Table S1, we designate all

breccias as “polymict breccias” unless there is petrographic evidence for one of the subcategories of Stöffler et al. (1980): fragmental breccia, regolith breccia, crystalline (impact) melt breccia, glassy (impact) melt breccia, or granulitic breccia.

To first order, compositions of breccias and soils from the Apollo sites and many brecciated lunar meteorites can be modeled as mixtures of lithologies of three extreme sorts, including (1) typical material from the FHT (feldspathic highlands terrane; Jolliff et al. 2000) with 3–5% FeO and low concentrations of incompatible elements like Sm and Th, (2) material from the PKT (Jolliff et al. 2000) with 8–12% FeO and high concentration of incompatible elements (e.g., $>3.5 \mu\text{g g}^{-1}$ Th), and (3) mare basalt typically with 17–23% FeO and moderately low concentrations of incompatible elements (Fig. 2; Fig. S3 in supporting information). As we demonstrate here, however, this simple three-component model fails for meteorites that contain mafic, high-Mg/Fe material that likely derives not from the maria but possibly the lower crust of the FHT or from the South Pole–Aitken Terrane, a mafic anomaly within the FHT that exposes material of the lower crust or even upper mantle (Jolliff et al. 2000). Many lunar meteorites from northern Africa are distinct from Apollo samples or lunar meteorites recovered from other locations. For example, about two-thirds are highly feldspathic ($<7\%$ FeO_T, Fig. 2). Apollo 16 was the only Apollo mission to obtain samples of the FHT distant from deposits of mare basalt, yet most feldspathic lunar meteorites lie outside the compositional range of Apollo 16 soils in having lower concentrations of incompatible elements (Fig. 2).

Certain elements and element ratios determined precisely by INAA ($\pm 2\%$) are particularly useful for addressing compositional differences among lunar meteorites. Concentrations of Sc range over a factor of 24 (compared to a factor of 10 for FeO, 7 for Al₂O₃, and 2 for CaO) among lunar meteorites and are a measure of the relative pyroxene abundance (Fig. 3). Cr/Sc (Fig. S4 in supporting information) is a proxy for Mg/Fe (Fig. 4; we do not determine MgO by INAA) and olivine/pyroxene (Fig. 5). Na and Eu concentrations reflect the mean albite composition of the plagioclase as well as the normative plagioclase abundance (Figs. S5 and S6 in supporting information; fig. 11 of Korotev et al. 2009; we do not determine Al₂O₃ by INAA). Relative abundances of REE (rare earth elements) vary widely among the meteorites (Fig. 6; Figs. S7–S14 in supporting information). Similarly, although both Sm and Th are incompatible elements that range over factors of 300 and 500 in concentration among lunar meteorites, Sm/Th varies by a factor of 10 and is a particularly useful discriminator

among KREEP-poor breccias (Fig. S15 in supporting information). Siderophile elements (Co, Ni, and Ir) are useful because some lunar meteorites contain more or different kinds of interplanetary (chondritic, iron) material than others (Warren et al. 1989; Puchtel et al. 2008; Fischer-Gödde et al. 2010). Finally, lunar meteorites from northern Africa are contaminated to varying degrees with terrestrial Na, P, K, Ca, As, Br, Sr, Ba, light REE (LREE), and U among elements determined by INAA. Barium, in particular, provides support that two stones did or did not share a common terrestrial climate history.

Our approach of analyzing multiple subsamples provides geologic information in that subsample data often define mixing trends on two-element plots (Fig. 7). The distribution of subsample data on such plots is also useful for establishing or rejecting pairing relationships. For example, compositional data for subsamples NEA (Northeast Africa) 001 and NWA 8046 overlap in Figs. 7b and 7d, but the distributions are substantially different. For some meteorites, there is little compositional spread among subsamples (Fig. 7a) while for others, the compositional spread is great (Fig. 7b–d). Unless stated otherwise, all uncertainties on averages stated here are 95% confidence limits based on the scatter of the subsample data. For most elements discussed here, sampling uncertainty considerably exceeds the analytical uncertainty (see NWA 5000 sawdust discussion in supporting information). We have experimented with using cluster analysis as an aid in establishing and rejecting pairing relationships and conclude that it is not particularly useful because, in fact, compositional data for subsamples of many meteorites do not actually cluster (Fig. 7).

For convenience in discussion, we sort the meteorites into nine categories on the basis of composition (Fig. 6) as (1) typical feldspathic breccias (27% of analyzed); (2) atypical feldspathic breccias (16%); (3) troctolitic breccias (4%); (4) KREEP-rich breccias (3%); (5) Apollo-16-like, feldspathic breccias (6%); (6) basaltic breccias (6%); (7) noritic and basalt-bearing feldspathic breccias (31%); (8) unbrecciated mare basalts (6%); and (9) the unique NWA 773 clan of breccias and igneous rocks (1%).

Typical Feldspathic Meteorites

We define “typical” feldspathic lunar meteorites as those for which the mass-weighted mean composition of the meteorite (or all stones of a presumed pair group) meets the following criteria: $<11 \mu\text{g g}^{-1}$ Sc (minimal mare material, $<10\%$; Fig. 6), $<1.5 \mu\text{g g}^{-1}$ Sm (minimal KREEP material, $<3\%$ Apollo 14 regolith equivalent; Fig. 6), Cr/Sc <100 (i.e., not troctolitic; Fig. 4), and

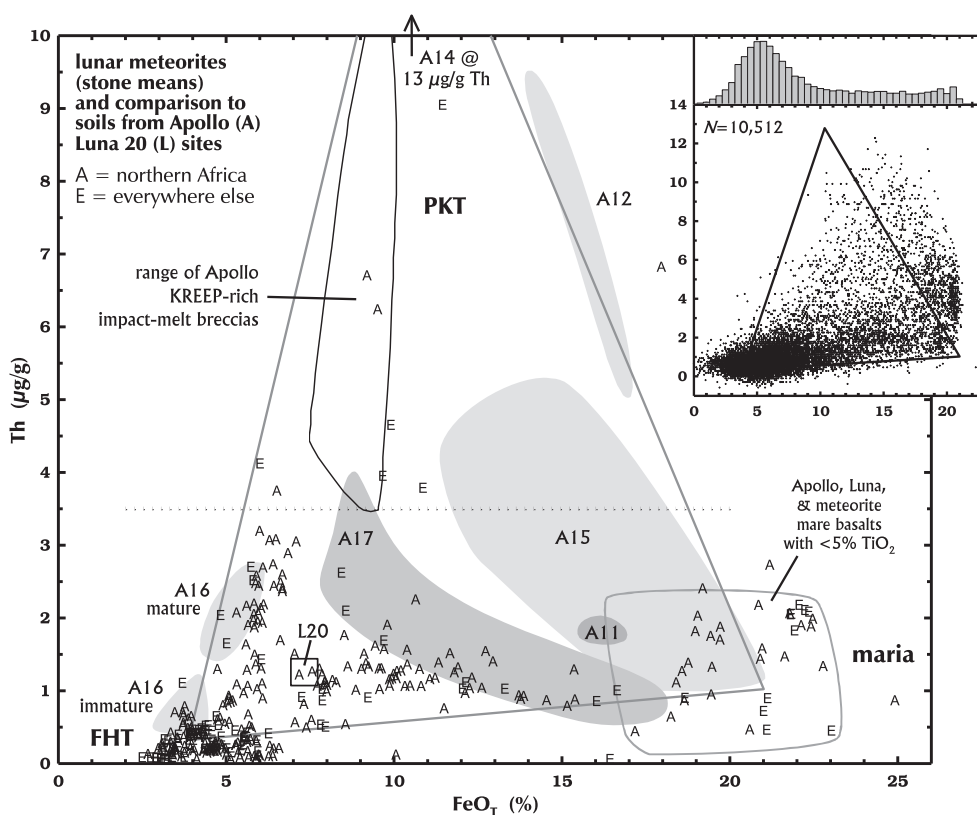


Fig. 2. Lunar meteorites in FeO_T–Th space (total Fe as FeO) with comparison to soils from the Apollo (“A11,” etc.) and Luna 20 (L20) sites and the range of Apollo KREEP-rich impact melt breccias (which extend off scale to 31 μg g^{−1} Th; Korotev 2000; Korotev et al. 2011). The two “A” points in this field are paired meteorites NWA 4472 and NWA 4475 (regolith breccias). Breccia Dhofar 1442 lies off scale at (14,15; Fig. S30a in supporting information). The inset depicts the 1° (30 km) gamma-ray spectrometer derived data from the Lunar Prospector mission (data of Lawrence et al. [2000], and Prettyman et al. [2006], with calibration of Gillis et al. [2004]). In the large figure, each “point” represents the mean composition of a lunar meteorite stone. The horizontal dotted line represents the FHT-PKT boundary of Jolliff et al. (2000). The large triangle is the mixing triangle of Korotev et al. (2003, fig. 6), Korotev (2005, fig. 17), and Korotev and Zeigler (2014, fig. 6.4), defined here by (1) the mean composition of typical feldspathic meteorites (Table S5 in supporting information), (2) the mean composition of six launch sites represented by the unbrecciated basaltic lunar meteorites (see text), and (3) somewhat arbitrarily, Apollo 14 soil representing the PKT (KREEP, off scale). Meteorite and mission data from this work, Hudgins et al. (2011a), Korotev (2005, 2012, 2017), Korotev et al. (2009), Korotev and Zeigler (2014), Lucey et al. (2006), Valencia et al. (2019), and references cited therein. See also Fig. S3.

0.30–0.40% Na₂O and 0.65–0.90 μg g^{−1} Eu (An_{97.5–96.6} in plagioclase; Figs. S5 and S16 in supporting information). Typical feldspathic meteorites have 3–5% FeO and, mineralogically, nearly all are noritic anorthosites, not anorthosites, on the basis of relative fractions of plagioclase, pyroxene, and olivine (Fig. 8). Twenty-one of the northern Africa meteorites are typical feldspathic meteorites that we suspect are unpaired with any others. In Figs. S17–S21 in supporting information, we provide the data and rationalization for these conclusions. In Table 2, we present a new estimate of the composition of the surface crust of the FHT distant from maria and the PKT based on typical feldspathic meteorites, including all those from elsewhere than northern Africa. The composition, corresponding to 86 vol% normative

plagioclase and $Mg' = 65.5$ (whole-rock mole% Mg/(Mg + Fe; Tables 2 and 3), is somewhat more feldspathic and more ferroan than previous estimates that were based on substantially fewer meteorites (Palme et al. 1991: 77% and 70; Korotev et al. 2003: 82% and 69; Table S5).

The typical feldspathic meteorites include both of the Libyan meteorites, regolith breccias DaG 262 and DaG 400 (Fig. S22 in supporting information), and two NWA clans for which there are many stones. The NWA 8222 clan (fragmental breccia) consists of eight stones totaling 28 kg (Fig. S23 in supporting information). Will et al. (2019) report no solar wind products in one of the stones, NWA 11237, so the rock is not a regolith breccia. We have analyzed 23 stones of the NWA 8046 clan (Fig. S24 in supporting information). We suspect on the

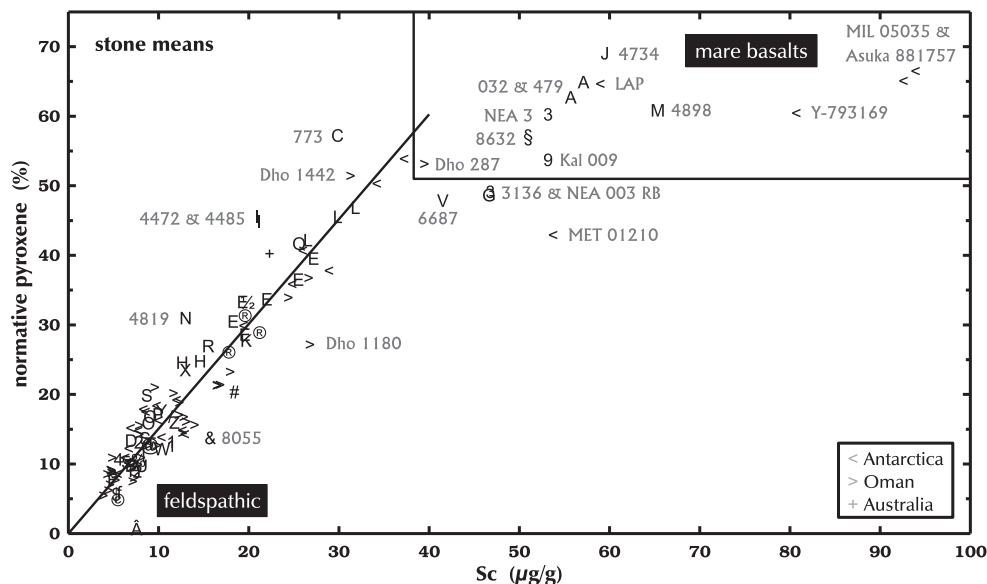


Fig. 3. Pyroxene is the major carrier of Sc in lunar samples; thus, Sc abundance is a proxy for pyroxene abundance and pyroxene/plagioclase, especially among feldspathic lunar meteorites. The line ($[\text{pyx}] = 1.51 \cdot [\text{Sc}]$) is defined by the origin and the mean of all points with $<40 \mu\text{g g}^{-1}$ Sc that are not labeled. Number-only labels are NWA stones. See Table S1 for symbol key for African meteorites.

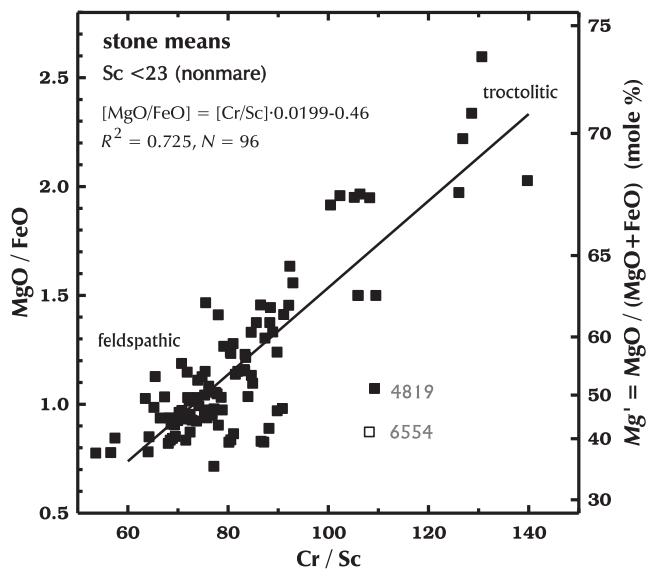


Fig. 4. Cr/Sc is a proxy for MgO/FeO (mass ratios) in nonmare lunar breccias. The diagonal line is a simple linear regression to the filled points, all representing the plagioclase-rich end of the Sc range of lunar meteorites ($<23 \mu\text{g g}^{-1}$ Sc, fig. 6). Updated from fig. 6 of Korotev (2005). Several subsamples of NWA 6554 are anomalously rich in Cr from spinel (Fig. S44g), so we have excluded this meteorite from the regression. NWA 4819 is also anomalously rich in Cr (Fig. S4). (Color figure can be viewed at wileyonlinelibrary.com.)

basis of petrography, MetBull descriptions, photos, and reported find location (near Tindouf, Algeria, but likely extending over a wide region and buried to variable

depths in the terrain), that at least another 19 stones are also part of the pair group (Table S1). The total mass of the 40 stones is 313 kg (including NWA 12760, the largest single lunar meteorite stone at 58 kg), making the NWA 8046 clan the largest lunar meteorite. From our review of the descriptions, we favor “feldspathic polymict breccia” as a description of the clan, although some stones are predominantly fragmental breccias or glassy matrix breccias. Only one glass spherule is reported among the 40 MetBull descriptions (NWA 2425), so the rock is marginally a regolith breccia (Stöffler et al. 1980). For clan member NWA 11273, Will et al. (2019) report a very low solar wind content. The meteorite is compositionally heterogeneous in part because it contains clasts of basalt (Fig. 7d; Fig. S24). Mg' is moderately high (72) in NWA 8046, consistent with the numerous troctolitic lithic clasts reported by Fagan and Gross (2020) for NWA 11303. Other lithic clasts include anorthosite, gabbro, basalt, granulite, impact melt breccia, and impact glass (MetBull; Treiman and Coleff 2018; Cao et al. 2019; Lunning and Gross 2019; Fagan and Gross 2020). Treiman and Semprich (2019) report a dunite clast ($\text{Fo}_{83.5}$) in NWA 11421. Most stones contain vesicular shock melt.

A characteristic of typical feldspathic meteorites is that, on average, they are less feldspathic ($\text{Al}_2\text{O}_3 = 29.6 \pm 0.6\%$, 95% confidence limits, equivalent to 82 wt% or 85 vol% plagioclase; Tables 3 and S5) than pristine ferroan anorthosites of the Apollo sites ($\text{Al}_2\text{O}_3 = 31.9 \pm 0.9\%$, equivalent to 88 wt% or 92 vol%

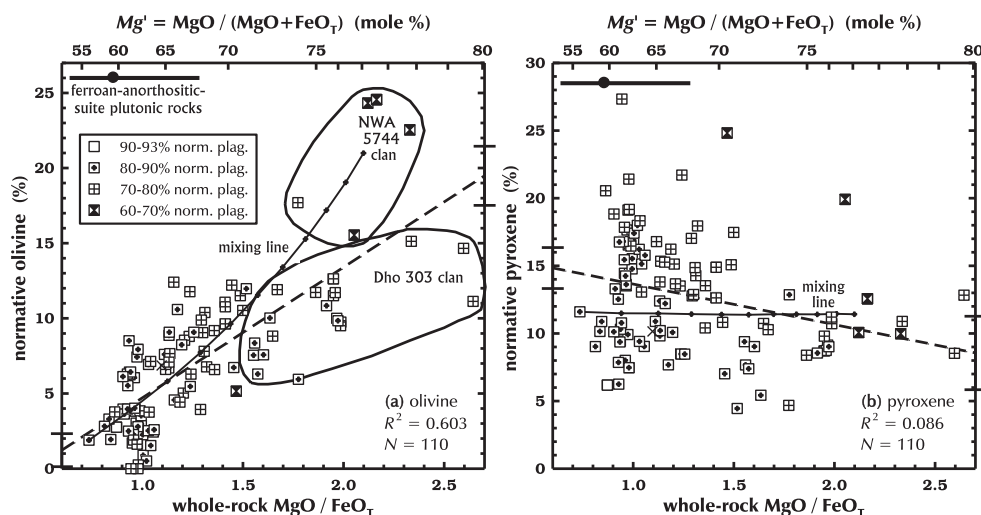


Fig. 5. Whole-rock major element data (110 analyses) for 77 lunar meteorite stones from the feldspathic highlands, all breccias with $<11 \mu\text{g g}^{-1}$ Sc (low mare component), $<3 \mu\text{g g}^{-1}$ Sm (low KREEP component), and $<300 \mu\text{g g}^{-1}$ Ni (minimal Fe and Mg from chondrites). Normative plagioclase ranges from 62% to 91% (approximately 67–93 vol%; CIPW normative mineralogy of Cross et al. [1902], calculated by the method of Johannsen [1931], via Excel® spreadsheet of Hollocher [2019]). a) High-MgO/FeO_T (total Fe as FeO) feldspathic lunar meteorites are rich in forsteritic olivine (updated from fig. 9 of Korotev et al. 2003). Low-MgO/FeO_T lunar meteorites tend to have only 0–7% normative olivine and Mg' in the range of FAS (ferroan-anorthositic-suite) plutonic rocks. The bar (upper left) representing the FAS shows the mean Mg' (circle), with standard deviation, of olivine and pyroxene in 41 pristine FAS suite samples of Warren (1993; pristinity “confidence class” ≥ 6.0). High-MgO/FeO_T feldspathic meteorites are troctolitic. Note that mixing lines between any ferroan, low-olivine meteorite (represented here by Oued Awlitis 001) and a magnesian, high-olivine meteorite (mean of five NWA 5744 clan points) is nonlinear. The dashed line represents simple linear regression; the error bars on the axis intercepts represent 95% confidence limits. b) There is little to no correlation between MgO/FeO and normative pyroxene abundance in the feldspathic highlands. Because of the simplicity of lunar mineralogy, the normative model rather accurately reflects average mineral proportions of the unbrecciated precursors of the breccias. Meteorite data are from Hudgins et al. (2011a), Joy et al. (2010), Kent et al. (2017), Korotev and Zeigler (2014), Korotev et al. (2009), Warren and Kallemeyn (1986, 1991), Warren et al. (2005), Zipfel et al. (1998), C. Agee and N. Muttik in MetBull (NWA 5744 pairs NWA 8687 and NWA 10140, melt veins), and this work.

plagioclase; Fig. 8). The difference is significant at the 99% confidence level (Welch’s *t*-test; Welch 1947). In the Apollo collection, most pristine ferroan anorthosites are from the Apollo 16 site; many are >100 g in mass and many are $>98\%$ plagioclase (Warren 1990). There is no evidence among typical feldspathic meteorites, however, that such plagioclase-rich rocks are common in the FHT. In subsampling of lunar meteorites for INAA, we deliberately prepared subsamples that were rich in “white clasts,” if available. The “purest” was an 8 mg subsample of a clast in NWA 3190 (bulk FeO = 9.2%) with only 0.20% FeO (Fig. 9b). Among all subsamples with $<10\%$ FeO ($N = 1678$), however, only 1.0% have less than 2.5% FeO, equivalent to 90 vol% plagioclase (Fig. 9b). In contrast, among more than 2000 lithic fragments that we have analyzed from the 1–2 mm and 2–4 mm grain size fractions of the Apollo 16 regolith samples (Fig. 9a), 18% of those with $<10\%$ FeO have $<2.5\%$ FeO. We suspect that the difference is a consequence of the Apollo 16 site being anomalously rich in highly feldspathic ($>90\%$ plagioclase) ferroan anorthosite compared to typical FHT material (Warren 1990; Korotev et al. 2003, 2010; Gross et al. 2014).

As noted by Gross et al. (2014), another characteristic of typical feldspathic meteorites is that they have a wide range of Mg' , 57–77 (Table S5), and, on average, they are more magnesian (mean Mg' in mafic silicates: 67 ± 2 ; Table 3) than pristine ferroan anorthosites of the Apollo collection (Mg' : 60.9 ± 2.4 ; Table 4; Fig. 10). Again, the difference is significant at the 99% confidence level (Welch’s *t*-test) and may reflect the sampling bias discussed above in that the ferroan anorthosites are not as common in lunar meteorites, and presumably the FHT as a whole, as they are at the Apollo 16 site. The Mg' variation reflects variation in olivine/pyroxene in the precursor noritic anorthosites of the meteorite breccias (Fig. 5). The wide range in Mg' also indicates that since formation of the feldspathic crust impact mixing has not homogenized the surface of the crust, that is, the crust was originally heterogeneous in Mg' and much of that heterogeneity has been preserved in the regolith.

The variation in Mg' in typical feldspathic meteorites does not correlate with simple igneous differentiation indices such as plagioclase composition or REE abundances (Fig. 11). The former might be

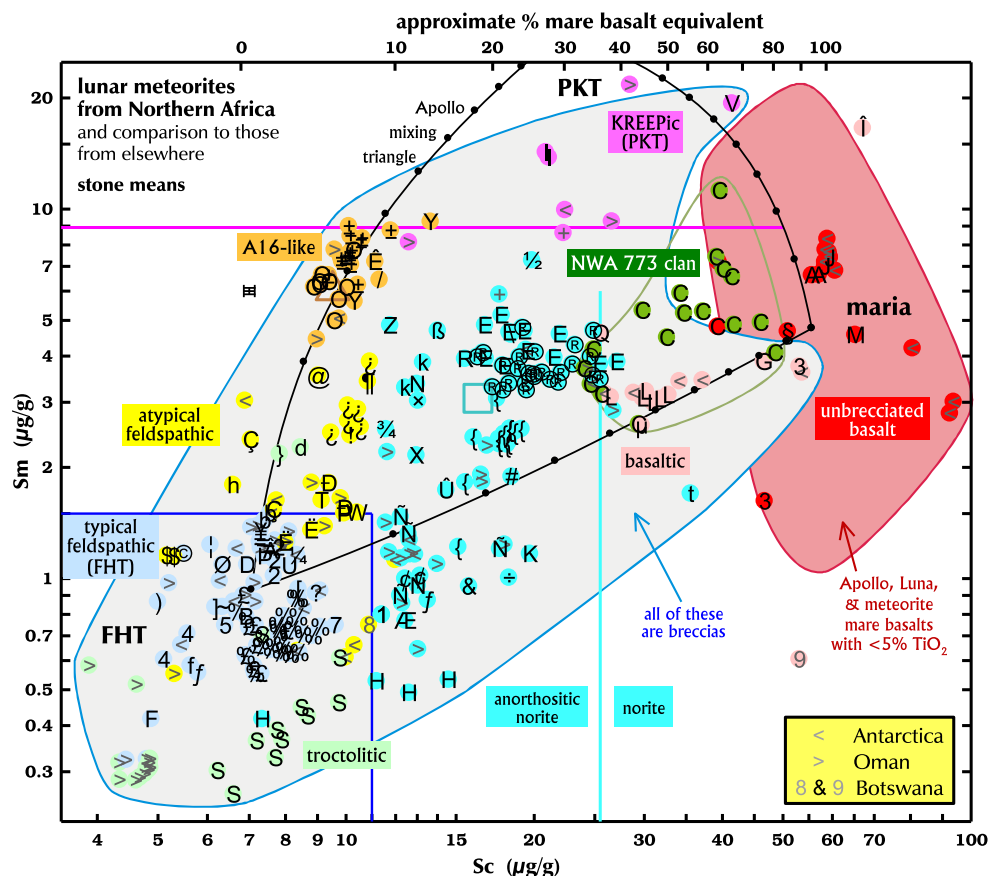


Fig. 6. Like Fig. 2 but in Sc-Sm space and with logarithmic axes (after Korotev et al. 2009). Lunar meteorites from northern Africa (stone means) are depicted by alphanumeric and “keyboard” symbols (symbol key in Table S1), with comparison to non-African meteorites (yellow legend) and the range of low- and very-low-Ti mare basalts. The red “C” in the NWA 773-clan field does not represent a meteorite stone but the olivine-phyric basalt lithology that dominates NWA 3160 and NWA 3333 of the NWA 773 clan. The horizontal line represents the FHT-PKT boundary of Jolliff et al. (2000), that is, $3.5 \mu\text{g g}^{-1} \text{Th} \times 2.55$, where 2.55 is the mean Sm/Th of KREEP-bearing impact melt breccias of the Apollo sites (Korotev 2000, Table 1). The curved lines depict the mixing triangle of Fig. 2. The small dots on the triangle represent 10% mixing increments. For example, the “A16-like” (Apollo 16) meteorites represent 70–90% typical FHT material mixed with 10–30% PKT material while NWA 6687 (symbol “V” at [41,19]) is a mixture of approximately 50% mare basalt and 50% PKT material with essentially no FHT material. The upper (mare basalt) axis applies only to those breccias that are, in fact, FHT-mare mixtures. As argued in the text, however, many of the “anorthositic norites” are breccias of anorthositic norite mineralogy with little mare material. Low-Sm ($<6 \mu\text{g g}^{-1}$) breccias with greater than about $25.5 \mu\text{g g}^{-1} \text{Sc}$ are norites (Fig. 8). For reference, the obscured triangle in the “A16-like” field represents the mean composition of typical Apollo 16 soils and the large square in the middle of the diagram represents the Luna 20 soil. These two landing sites are in feldspathic highlands distant from maria but, clearly, neither is typical of the FHT. The error bars (under “A16-like” label) represent $\pm 2\sigma$ analytical uncertainties.

expected in that a characteristic of ferroan-anorthositic-suite rocks is that An (mole% $\text{Ca}/[\text{Ca} + \text{Na}]$) is largely invariant with varying Mg' of the coexisting mafic silicates (e.g., Raedeke and McCallum 1980; Warren and Wasson 1980; Pernet-Fisher et al. 2019). Our observation, however, is based on whole-rock analyses of breccias and supports conclusions based on mineral compositions in feldspathic lunar meteorites (Arai et al. 2008; Gross et al. 2014; Russell et al. 2014; Pernet-Fisher et al. 2019): The precursor anorthosites of these breccias did not all crystallize from a common magma. Bulk compositions of typical feldspathic meteorites are

more consistent with models in which the precursor plutonic rocks are products of processes more complex than simple flotation of plagioclase in a magma ocean (Longhi 2003; Gross et al. 2014; Xu et al. 2020). These processes led to regional differences in olivine/pyroxene and, consequently, Mg' (Arai et al. 2008; Ohtake et al. 2012) in the early feldspathic crust.

Atypical Feldspathic Meteorites

Na/Eu is nearly constant in feldspathic lunar rocks because both elements occur almost exclusively in

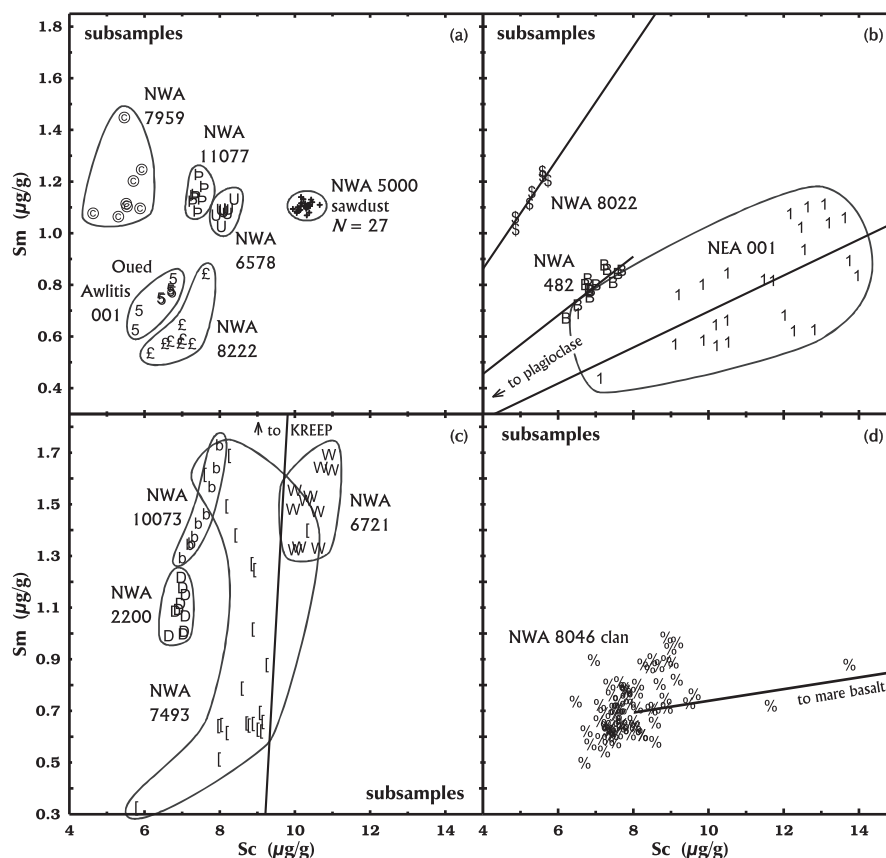


Fig. 7. All meteorites of this figure are feldspathic, KREEP-poor breccias (Fig. 6). a) This panel shows some meteorites with minimal compositional variation among subsamples. Nevertheless, subsamples of chips and fines (30 ± 5 mg each, mean and standard deviation) vary in composition considerably more than do subsamples of NWA 5000 sawdust (supporting information) of approximately the same mass (for the sawdust, actual Sm concentrations are $2\times$ greater than plotted here). See supporting information on details of the sawdust analyses. b) Subsamples of NEA 001 vary over a considerably greater range of compositions than the meteorites of (a). In the meteorites of this panel, the variation is mainly due to differences in the pyroxene to plagioclase ratio among subsamples, sometimes associated with plagioclase-rich clasts in a more mafic matrix. The diagonal lines are defined by the origin (i.e., pure plagioclase) and the means of the NWA 8022, NWA 482, and NEA 001 subsamples. The mixing trends in these meteorites are effectively “plagioclase dilution” trends. c) For many feldspathic meteorites, Sc concentrations are rather constant but concentrations of incompatible elements vary because of variable relative abundance of some KREEP lithology in the breccias. d) Finally, some feldspathic breccias contain nuggets of mare basalt that lead to high concentrations of Sc, Cr, and Fe in some subsamples (see also Fig. S24).

plagioclase. For example, Na/Eu ranges from 3100 to 3700 among the typical feldspathic meteorites. For comparison, Na/Eu ranges from 2000 to 2500 among mafic, KREEP-rich impact melt breccias of the Apollo collection and is typically ~ 1900 in Apollo alkali anorthosite (Korotev 2000; Korotev et al. 2011). Among the mare basalts of this study, the range is 2200–3400 (e.g., Fig. 6).

Atypical feldspathic meteorites ($N = 12$) differ from the typical feldspathic meteorites only in having (1) greater concentrations of Na_2O (0.4–0.5%) or Eu (0.90 – $1.15 \mu\text{g g}^{-1}$, $N = 7$, Fig. S16) or (2) greater concentrations of Sm (1.5 – $4.0 \mu\text{g g}^{-1}$, Fig. 6; Fig. S25 in supporting information). The latter leads to some negative Eu anomalies (Fig. S9). For NWA 8001, NWA

10404, NWA 10678, Rabt Sbayta 007, and Talhat Lihoudi (Na/Eu: 3100–3300), the excess Na, Sm, and Eu are largely consistent with a mixture of typical feldspathic meteorite and a small component (3–9%, Fig. S6) of some PKT lithology. The high Sm concentrations of the NWA 8641 and NWA 10783 clans (Fig. S26 in supporting information) are likely also caused by a small (6–9%) PKT component. For these two meteorites, as well as NWA 5000 and NWA 6481, Eu/Sm and Na/Sm considerably exceed the KREEP ratio. The anomaly appears to be mainly caused by plagioclase more albitic than the Ab_3 typical of feldspathic meteorites. NWA 8022/10082, the most feldspathic of the atypical feldspathic meteorites, also has anomalously high Na and Eu but no KREEP

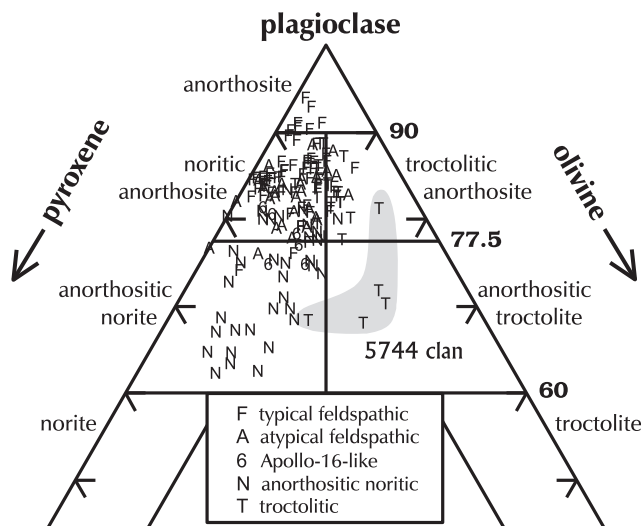


Fig. 8. Plagioclase-rich apex of the classification diagram for igneous and plutonic rocks of the lunar highlands (Stöffler et al. 1980) and distribution of feldspathic to moderately mafic ($<12\%$ FeO_T , $<25 \mu\text{g g}^{-1}$ Sc, $<8 \mu\text{g g}^{-1}$ Sm) lunar meteorites, all breccias, for which there are major element data. Each point represents an analysis and the letter symbols refer to compositional types of Fig. 6. Most feldspathic lunar meteorites, and presumably the upper feldspathic crust of the Moon, derive from noritic anorthosites. Troctolitic meteorites (Fig. 5) are rare, as are anorthosites with >90 vol% plagioclase. Two of the 5744 clan points are based on electron probe analysis of “shock melt” in NWA 8687 and NWA 10140 by C. Agee and N. Muttik (MetBull). For this plot, we used the Excel® spreadsheet of Hollocher (2019) to calculate normative volume percent of each mineral from the major element compositions (sources of Fig. 5) and normalized the sum of plagioclase, olivine, and pyroxenes to 100%. The basaltic and “KREEPic” breccias of Fig. 6 largely plot in the norite field.

component (Figs. S5, S16, and S25). Plagioclase more albitic than the Ab_3 typical of ferroan anorthosite has been reported from both Apollo rocks and other feldspathic lunar meteorites (James et al. 1989; Nyquist et al. 2006; Yamaguchi et al. 2010; Korotev 2012).

NWA 6721 is anomalous in having a high Na_2O concentration ($0.47 \pm 0.02\%$), but an Eu concentration that is typical of the feldspathic meteorites, leading to a high Na/Eu (4000; Figs. S6 and S25b,e). We suspect the meteorite to be contaminated with terrestrial Na as it also has a high concentration of terrestrial Br, $1.7 \mu\text{g g}^{-1}$. NWA 11223/11809 is anomalous because it is contaminated with terrestrial REE, including Eu (below).

Atypical feldspathic meteorites include 11.5 kg NWA 5000, a metal-rich fragmental breccia (Figs. S27 and S28 in supporting information). The breccia is dominated by clasts of impact melt breccia of gabbroanorthite mineralogy and texture (Irving et al. 2008; Nagurney et al. 2016). Consequently, the meteorite has

Table 2. Mean composition of 24 typical feldspathic lunar meteorites as an estimate of the typical composition of the surface of the feldspathic highlands terrane.

	Unit	Mean	\pm
SiO_2	wt%	44.24	0.19
TiO_2	wt%	0.184	0.017
Al_2O_3	wt%	29.6	0.6
Cr_2O_3	wt%	0.080	0.005
FeO_T	wt%	3.82	0.18
MnO	wt%	0.061	0.005
MgO	wt%	4.33	0.57
CaO	wt%	16.8	0.3
Na_2O	wt%	0.343	0.007
K_2O	wt%	0.028	0.004
P_2O_5	wt%	0.029	0.006
Σ	wt%	99.5	
Mg'	mol%	65.5	2.1

Note: FeO_T = Total Fe as FeO. $\text{Mg}' = \text{MgO}/(\text{MgO} + \text{FeO})$.

Uncertainties (\pm) are 95% confidence limits. See Table S5 for trace element data and details.

Table 3. Normative mineralogy of typical feldspathic lunar meteorites (FLM).

Mineral	FLM mass %		FLM vol%	
	Mean	Range	Mean	Range
Plagioclase	81.9	71–88	85.1	75–90
Orthoclase	0.18	0.12–0.24	0.20	0.13–0.27
Pyroxene	11.6	5–19	9.72	4–17
Diopside	3.1	0–6	2.65	0–5
Hypersthene	8.5	0–15	7.1	0–13
Olivine	5.63	2–12	4.47	1.5–10
Ilmenite	0.34	0.13–0.49	0.21	0.08–0.30
Apatite	0.07	0.05–0.12	0.06	0.04–0.10
Chromite	0.12	0.09–0.19	0.07	0.05–0.11
Sum	99.9		99.8	
An in plagioclase	97.1	96.7–97.6	97.1	96.7–97.6
Mafic silicates	17	12–28	14	9–24
Mg' in mafic silicates ^a	67 ± 2	58–78	67 ± 2	58–78
Ol/(Ol + Py)	33	10–72	32	10–70

Note: Values in %. Results based on major element data of Table S5 for 24 typical FLMs and Excel® spreadsheet of Hollocher (2019).

^a Mg' here is slightly greater than the 65.5 of Table 2, which is a “whole rock” value that includes ilmenite.

been described as a monomict breccia because all the large clasts are the same lithology. Matrix-rich subsamples and sawdust from cutting of the rock are distinctly richer than the clasts in incompatible elements and Na_2O , however, suggesting a finer grained matrix component (regolith?). The bulk composition of the NWA 5000 matrix is equivalent to a 1:1 mixture of the gabbroanorthite clasts and a material with a composition like the NWA 8641 clan (Fig. S29 in supporting information), suggesting possible launch pairing.

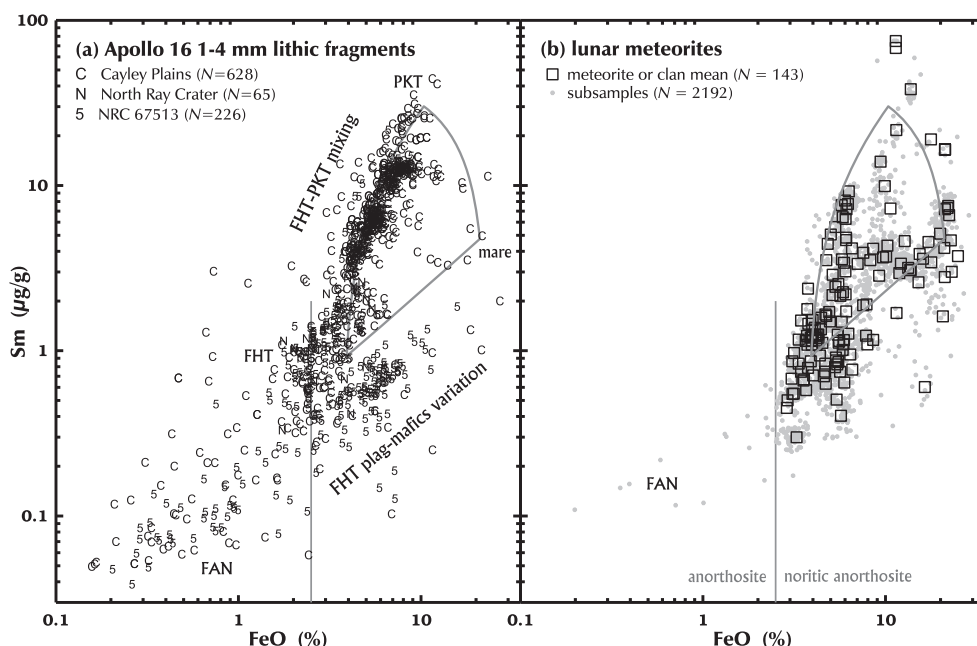


Fig. 9. Comparison of Apollo 16 lithologies to lunar meteorites in FeO-Sm space. a) Lithic fragments from the 1–2 mm and 2–4 mm grain size fractions of Apollo 16 regolith samples (mean mass each: 15 mg) and comparison to the mixing triangles of Figs. 2 and 6. The “N” symbols represent samples from station 7 at North Ray Crater, “5” symbols represent mafic North Ray Crater sample 67513 (Jolliff and Haskin 1995), and “C” symbols represent soils from the Cayley Plains at the central and southern sampling stations. Mineralogically, fragments with less than ~2.5% FeO (vertical line) are anorthosites (Fig. 8) or impact glasses derived therefrom. Of the fragments with < 10% FeO, 18% plot in the FAN (ferroan anorthosite) field. Nearly all of the numerous Apollo 16 fragments with 2.5–50 $\mu\text{g g}^{-1}$ Sm that plot along the FHT-PKT join are impact melt breccias and glass composed of KREEPy melt and feldspathic clasts (Korotev 1987). The low-Sm fragments of 67513 derive from a KREEP-free noritic anorthosite pluton and the trend (0.2–20% FeO) represents variable plagioclase/pyroxene among the small fragments (Jolliff and Haskin 1995). Other data are from the “Apollo 16 comparison suite” of Korotev et al. (2003). b) Each square point represents a lunar meteorite, that is, all stones of a presumed pair group or clan are represented by one point except dilithologic meteorites (e.g., NEA 003) are represented by two points. The small gray points are all subsample data for the same suite of meteorites (mean mass: 30 mg). Note that compared to Apollo 16 (a), ferroan anorthosite (FAN) is not abundant in the lunar meteorites, only 1.0% of subsamples with <10% FeO. Data from Korotev (2012, 2017), Korotev and Zeigler (2014), and this work.

Troctolitic Meteorites

Highly magnesian (high Mg') feldspathic breccias are not common in the Apollo collection. Most such Apollo rocks are granulitic breccias from Apollo 16 and 17 (Lindstrom and Lindstrom 1986). The Dhofar 303 clan of lunar meteorites from Oman comprises 16 stones (total mass: 1.0 kg), all impact melt breccias with troctolitic–anorthosite mineralogy and composition, that is, 74–85% normative plagioclase (~77–89 vol%), 6–15% normative olivine (~5–13 vol%), 5–13% normative pyroxene (~5–11 vol%), and Mg' averaging 77 (Takeda et al. 2006; Demidova et al. 2007; Treiman et al. 2010; Korotev 2012, 2017). These values compare with 88% modal plagioclase and 12% modal olivine (Fo_{87}) in Apollo 17 unbrecciated troctolitic–anorthosite sample 76335 (Warren and Wasson 1977).

Even more mafic is one of the most distinct lunar meteorites from northern Africa, the NWA 5744 clan of

granulitic breccias with anorthositic troctolite mineralogy (8 stones of 2.5 kg mass; Kuehner et al. 2010; Hilton et al. 2016; Kent et al. 2017; Robinson and Kring 2018; Gross et al. 2020; see Fig. S1f for a photo of one of the distinct stones, NWA 8687). Modal data are available for three of the stones: 59–75% plagioclase (An_{96-98}), 15–26% olivine (Fo_{77-80}), and 3–15% pyroxenes (NWA 8687 and 10140, C. Agee, *MetBull*; NWA 10401, Gross et al. 2020). These values compare with 50–60% plagioclase, 35–37% olivine (Fo_{87}), and 4–5% orthopyroxene in Apollo 17 unbrecciated troctolite 76535 (Gooley et al. 1974; Dymek et al. 1975; Warren 1993). One of the stones, NWA 10318, is not an anorthositic troctolite, but a “granulitic breccia of olivine-bearing anorthositic norite precursor” (A. Bischoff and S. Ebert in *MetBull*). We suspect that NWA 10318 is, nevertheless, a member of the NWA 5744 clan because it plots at the Sc-rich (i.e., pyroxene-rich) end of the trends for subsamples of the clan (Fig. S30a in supporting information).

Table 4. Estimated number of lunar meteorites and lunar-meteorite launch sites (December 31, 2019).

	Antarctica	Australia	Oman	Saudi Arabia	Botswana	Northern Africa	Total
Number of stones	40	2	71	2	2	281	398
Number of characterized stones ^a	40	2	70	2	2	225	341
Among characterized stones, preferred number of meteorites	23	2	28	2	1	84	140
Minimum	23	2	27	2	1	77	131
Maximum	23	2	29	2	1	91	147
Minimum number of launch sites							109
Maximum number of launch sites							134

Note: See Table S7 in supporting information for details. Note that 13% of the stones have not been chemically analyzed.

Likely launch-pair groups (**bold**: first or most prominent member of launch-pair group). (1) YAMM: **Y-793169**, Asuka 881757, MET 01210, and MIL 050035; (2) YQEND: **Y-793274/981031**, QUE 94281, EET 87521/96008, NWA 4884, NWA 7611 clan ($N = 5$), DEW 12007, and the DOM 18xxx stones (no compositional data yet); (3) NNL: **NWA 032/10597**, NWA 4734/10597, LAP 02205 clan ($N = 6$), and possibly NWA 12008 and 12839; (4) **Dhofar 925** clan ($N = 3$), SaU 449, and NWA 8673 clan ($N = 14$); (5) **NWA 8455** clan ($N = 15$) and Dhofar 1627.

Possible launch-pair groups (**bold**: first or most prominent member of launch-pair group). (6) **MIL 090036** and NWA 7022; (7) **Y-791197** and MIL 07006; (8) **NWA 8641 clan** ($N = 6$), NWA 5000, and NWA 10783; (9) **NWA 10141 clan** ($N = 3$) and NWA 11077; (10) **NWA 10509 clan** ($N = 6$) and NWA 10626.

^aMostly based on chemical composition but includes 8 petrographically (AP 007, Dho 909, NWA 12393, NWA 12839, NWA 11767, NWA 12971, and NWA 12997) and 12 geographically identifiable meteorites (DaG 1048, Dho 460, Dho 1224, DOM 18262 and four pairs, NWA 12760, Rabt Sbayta 005 and 006, and Swayyah 001).

The NWA 5744 clan is compositionally unique in being magnesian and having lower concentrations of incompatible elements like Sm ($0.26\text{--}0.70\text{ }\mu\text{g g}^{-1}$; Fig. 6) than the otherwise similar feldspathic and magnesian granulitic breccias of the Apollo collection ($1\text{--}2.5\text{ }\mu\text{g g}^{-1}$, fig. 16 of Korotev et al. 2003). The mean CI-chondrite-normalized Sm/Th (0.91 ± 0.11) is nearly chondritic and distinctly greater than that of typical feldspathic meteorites (0.59 ± 0.03 ; Figs. S15 and S30e). The same is also largely true of Sm/Lu (Fig. S7) because in these moderately mafic rocks and in the absence of a KREEP component, the heavy REE are carried mainly by pyroxenes, which have greater relative concentrations of heavy REE than light REE (e.g., Lindstrom et al. 1984; Fig. 6). For example, for one of these meteorites, NWA 10401, 86% of the La and 46% of the Sm are carried by plagioclase while 92% and 95% of the Yb and Lu are contributed by pyroxenes (79–82%) and olivine (10–15%; from data of Gross et al. 2020). The importance of the NWA 5744 clan is that it represents olivine-rich, magnesian feldspathic crust distant from the PKT. It may represent deep crust of the FHT (Takeda et al. 2006; Kent et al. 2017) or possibly differentiated impact melt with both troctolitic and noritic (NWA 10318) components. On average, Ir concentrations in the NWA 5744 clan average 1.8 ng g^{-1} , which corresponds to 0.3% CM chondrite, at the low end of the range for brecciated lunar meteorites (Fig. 12, symbols “S”).

On the basis of high Cr/Sc and low CaO/FeO, we suspect that Aridal 017, NWA 11851, and a mafic clast that dominate our sample of NWA 11182 (Fig. S1h) may also be troctolitic. Boyle et al. (2018), however, did not observe any mafic, magnesian lithologies in their

thin section of NWA 11182, but they did observe olivine-bearing anorthosites.

Magnesium and Olivine in the Feldspathic Highlands

MgO/FeO of the lunar crust, its variation laterally and with depth, and the mineralogical control on MgO/FeO provide fundamental constraints on lunar crust–mantle differentiation (Warren 1986a, 1986b; Ohtake et al. 2012; Charlier et al. 2018; Lemelin et al. 2019). Interest in olivine in the feldspathic highlands has increased with better techniques for determining its abundance from orbit (e.g., Yamamoto et al. 2010; Ohtake et al. 2012; Crites and Lucey 2015; Arnold et al. 2016). We make some observations from lunar meteorites that provide constraints on differentiation models and interpretation of orbital data.

Among feldspathic lunar meteorites (those with >60% plagioclase), there is a tendency for the normative abundance of olivine to increase with increasing whole-rock MgO/FeO (Fig. 5a). In contrast, there is no correlation between whole-rock MgO/FeO and normative pyroxene (Fig. 5b). Thus, high-MgO/FeO in feldspathic rocks of the lunar highlands is largely dependent on the relative abundance of olivine of $\text{Fo}_{>75}$ composition. Those meteorites with the lowest MgO/FeO have Mg' (<65) in the range of the ferroan-anorthositic-suite of plutonic rocks (Warren 1993), have little normative olivine (2–7%), and are feldspathic (mean normative plagioclase: 82%). All of those with Mg' greater than the range of most ferroan-anorthositic-suite plutonic rocks have moderate abundances of normative olivine (10–25%) and tend to be more mafic overall (mean plagioclase: 72%).

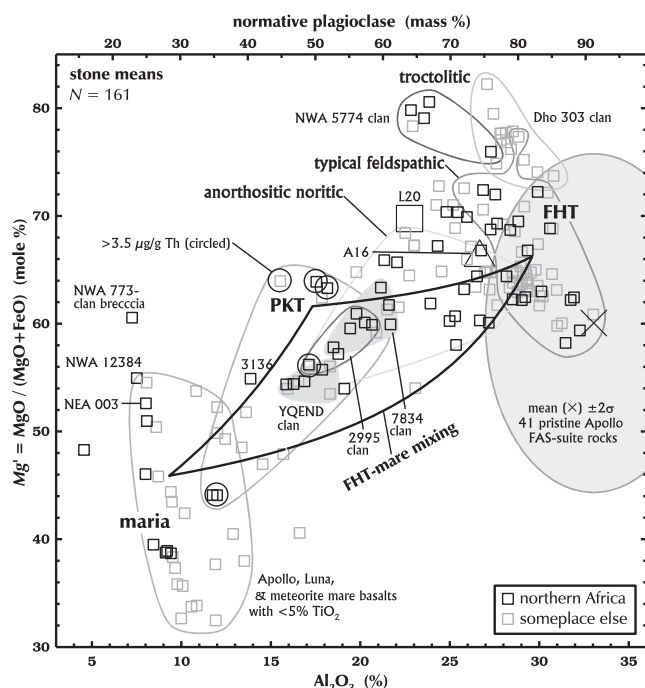


Fig. 10. Both basaltic and feldspathic lunar meteorites vary considerably in Mg' . The solid-line distorted “triangle” is the mixing triangle of Figs. 2 and 6. The FHT apex is defined by the mean of 24 typical feldspathic meteorites in the FHT field (Table S5). The truncated shaded ellipse on the right represents the pristine FAS (ferroan-anorthositic-suite) rocks of Warren (1993; “confidence class” ≥ 6.0). Most typical feldspathic meteorites are both less feldspathic and more magnesian (greater Mg') than typical FAS rocks (see also Fig. 5), indicating that some must contain a high- Mg' , troctolitic lithology like those of the Dhofar 303 and NWA 5744 lunar meteorite clans. Similarly, most lunar meteorites that are more mafic than the typical feldspathic meteorites, for example, the anorthositic-noritic field, are more magnesian than mixtures of typical FHT material and typical mare basalt (base of “triangle”). These rocks must also contain a substantial component of magnesian, nonmare material. Note that (1) few meteorites with $< 80\%$ normative feldspar plot near the FHT-maria join of the triangle and (2) both NWA 3136 and the YQEND launch pairs (Fig. S41), which plot on the FHT-maria join of Fig. 6 (i.e., minimal PKT material), are both more magnesian ($Mg' \sim 55$) than the FHT-maria join ($Mg' \sim 45$). This characteristic is also true of the NWA 2995 and NWA 7834 clans. All, however, are consistent with either a basalt component that is considerably more magnesian than the model basalt component or, more likely, typical basalt plus a mafic, high- Mg' nonmare component. Overall, this plot demonstrates that the ternary model of Figs. 2 and 6 is inadequate in that a fourth, high- Mg' (and high Cr/Sc; Fig. 4), nonmare component is also required. Updated from fig. 9 of Korotev et al. (2003) and fig. 6 of Korotev (2005). See also fig. 11 of Kent et al. (2017). Sources of data: those of Fig. 5, Carpenter et al. (2019), and Cohen et al. (2019).

Perhaps counterintuitively, FeO concentrations in the feldspathic meteorites of Fig. 5 range from 2.50% to 6.05%, a factor of only 2.4, whereas MgO

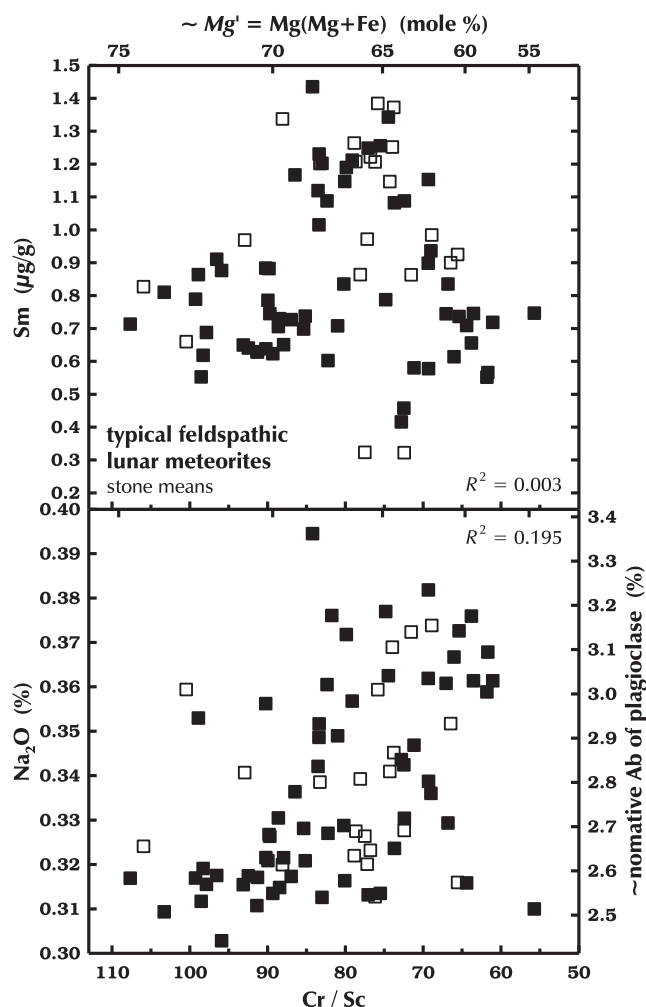


Fig. 11. Filled squares represent meteorites from northern Africa; open squares represent meteorites from Oman and Antarctica. The Mg' scale is based on the calibration of Fig. 4. Normative plagioclase ranges from 71% to 88% (mean: 82%) among the 84 stones of the figure. a) We define “typical feldspathic” meteorites as those meteorites with $< 1.5 \mu\text{g g}^{-1}$ Sm, that is, insignificant KREEP component. Among such meteorites, there is no increase in Sm concentration with decreasing Cr/Sc or Mg' , as we might expect if the wide range in Mg' results from differentiation of a common magma. b) There is only a weak tendency for the normative albite component of the plagioclase to increase with decreasing Mg' , at most from $Ab_{2.5}$ to $Ab_{3.5}$. Note that we have also defined “typical feldspathic” as those meteorites with 0.3–0.4% Na_2O , so this plot does not include those feldspathic meteorites with anomalously high concentrations of sodium (Fig. S25).

concentrations in the same rocks range from 2.2 to 12.9%, a factor of 5.9. Thus, if the feldspathic meteorites reflect the composition and mineralogy of the FHT as observed from orbiting spacecraft (e.g., Corley et al. 2018), then FeO abundances derived from pyroxene absorption bands are by themselves not necessarily good

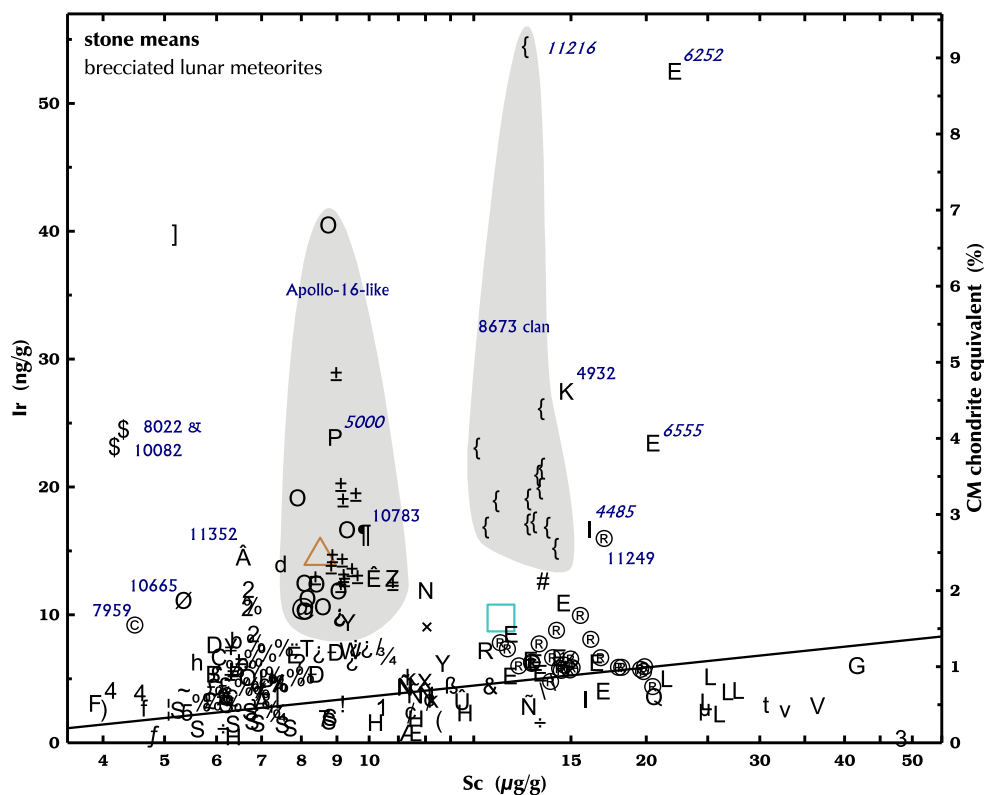


Fig. 12. Iridium concentrations in brecciated lunar meteorites from northern Africa. For the low-Ir meteorites, most Ir derives from micrometeorites, mainly CM chondrites in the regolith breccias (Wasson et al. 1975). Most lunar meteorites have Ir concentrations equivalent to <1.5% CM chondrites. All high-Ir lunar meteorites are rich in FeNi metal and all stones labeled in italics are high in Ir only because one or two subsamples contain large grains of FeNi metal, for example, 172 ng g⁻¹ in one subsample of NWA 11216. One subsample of NWA 6252 with 157 ng g⁻¹ Ir (off scale) contains an OsIrRuMoPt-alloy nugget from a calcium aluminum inclusion (Fig. S36). The large triangle represents Apollo 16 soil and the large square represents Luna 20 soil. The diagonal line represents the typical detection limit (3σ) for Ir in single subsamples. Because each point represents the weighted mean of several subsamples, however, points lying beneath the line are likely more significant than the line implies. See Table S1 for symbol key. (Color figure can be viewed at wileyonlinelibrary.com.)

indicators of how mafic a region is. For example, of that portion of the FeO carried by pyroxene and olivine (~90% for most feldspathic breccias), in a typical feldspathic meteorite (mean, 3.9% FeO, Table S5), 44% is carried by olivine and 56% by pyroxene whereas for the NWA 5744 clan of anorthositic troctolites (5.9% FeO, Table S5), 72% of the FeO is carried by olivine and only 28% by pyroxene.

The typical feldspathic meteorites provide the best estimate of Mg' for the surface of the FHT: 65.5 ± 2.1 (Table 2; Table S5). This value is greater than either the lunar nearside (55.4) or farside (63.3) values estimated from the Kaguya Spectral Profiler data (Ohtake et al. 2012). Similarly, Mg' for mature soil from the Apollo 16 site, 66.5 ± 0.6 (Korotev 1997) is considerably greater than the $Mg' = 61.6$ estimated for the Apollo 16 landing site by Ohtake et al. (2012). Curiously, Ohtake et al. (2012) equate their Mg' value for Apollo 16 with the value for ferroan anorthosite. Simple consideration of mass balance, however, shows that only 33% and 35% of

the FeO and MgO in mature Apollo 16 soil derive from rocks of the FHT (components 3, 4, and 6 of table 7 of Korotev 1997), while 41% and 49% derive from KREEP-rich, mafic, impact melt breccias from the PKT and a non-negligible 22% and 13% derive from the maria. These estimates assume that the mafic impact melt breccias are themselves mixtures of 75% PKT material ("pure" KREEP) with 10.3% FeO ($Mg' = 70.5$) and 25% FHT material (largely as clasts) with 2.5% FeO ($Mg' = 68$; calculated from data of table 7 of Korotev 1997). The interpretations of Ohtake et al. (2012) ignore the fact that most of the surface of the nearside FHT, and certainly the Apollo 16 site, is contaminated with moderately magnesian Imbrium ejecta (Haskin 1998).

KREEP-Rich Meteorites

Two lunar meteorites from northern Africa have concentrations of incompatible elements sufficiently great that they likely originate from the PKT. Paired

stones NWA 4472 and NWA 4485 ([FeO,Th] = [9,7] in Fig. 2) are high-silica (Fig. S31 in supporting information) regolith breccias consisting of material from all three apices of the mixing triangles of Figs. 2 and 6. Lithic clasts include granulitic breccia, Mg-rich impact melt breccia, KREEP basalt, and very-low-Ti mare basalt (Arai et al. 2009; Joy et al. 2011). The meteorite must also contain some basalt with >1% TiO₂ because the breccias contain 1.2% TiO₂ (Fig. S32 in supporting information). One of our subsamples of NWA 4472 contains a 0.2 mg grain of RE-merrillite and one subsample of NWA 4485 contains a 9 mg nugget of FeNi metal (Fig. S33 in supporting information).

Largely undescribed, NWA 6687 ([18,7] in Fig. S26) is a PKT-mare mixture with minimal FHT material and a composition similar to that of Apollo 12 soils; we discuss this meteorite in more detail below. With 9 $\mu\text{g g}^{-1}$ Sm, the large melt-breccia clast that dominates NWA 7022 likely also originates from the PKT. This meteorite may be launch paired with MIL 090036 (Miller Range, Antarctica; Fig. S34 in supporting information).

Apollo-16-Like, Feldspathic Meteorites

The first three lunar meteorites to be recognized, Allan Hills A81005, Yamato 791197, and paired stones Yamato 82192/3, are all feldspathic regolith breccias. In the late 1980s, geochemists noted (1) that all three differed from soils and most feldspathic rocks from the Apollo 16 highlands in having lower concentrations of elements associated with KREEP and (2) that the difference likely indicated that all three meteorites originated from places on the Moon distant from the Apollo sites, perhaps the farside (Bischoff et al. 1986; Fukuoka et al. 1986; Lindstrom et al. 1986; Ostertag et al. 1986; Warren and Kallemeyn 1986; Koeberl 1988; Koeberl et al. 1989).

The first lunar meteorite with a composition similar to that of Apollo 16 soil, NWA 4936, was not recognized until 2008 (Korotev et al. 2008). Since then, seven others have been found that together with the NWA 4936 clan represent as many as six different launch sites on the Moon (Fig. S35 in supporting information). The NWA 4936 clan (9 stones, 1.9 kg), the NWA 8455 clan (15 stones, >7.0 kg), NWA 8010 (1 stone, 58 g), NWA 10973 (1 stone, 25 g), and the Dhofar 1627 clan (2 stones, 110 g) are not only similar to Apollo 16 regolith in terms of moderately high lithophile element concentrations but also high concentrations of Ni and Ir and similarly non-chondritic Ir/Ni (Figs. S35e,f, S36a, and S37 in supporting information). The other three Apollo-16-like meteorites, NWA 7022 (1 stone, 444 g),

NWA 7274 (1 stone, 373 g), and MIL 090036 (1 stone, 245 g), have low concentrations of siderophile elements and more nearly chondritic Ir/Ni (Fig. S35e,f). In terms of the three-component model of Figs. 2 and 6, all of these meteorites (like Apollo 16 soils; Korotev 1997) are mainly FHT-PKT impact mixtures with varying but small amounts (<10%) of admixed mare material (Fig. S32). Proportions of the PKT (KREEP) component also vary among the six launch sites. If we assume that Apollo 14 soil represents the PKT component (30 $\mu\text{g g}^{-1}$ Th and 13 $\mu\text{g g}^{-1}$ Sm, as depicted by the triangle of Fig. and 6), then the PKT:FHT proportions range from 13:87 to 21:79 among the six launch sites (mean 16:88).

If these meteorites represent as many as six different launch sites, why do they all cluster near the Apollo 16 field on Figs. 2 and 6 and why do four of the six have nonchondritic Ni/Ir, similar to Apollo 16 soil (Fig. S35)? Why do the NWA 4936 clan, 8455 clan, NWA 7022, and NWA 8022 (TiO₂ not measured in the others) have a similar relative abundance of mare basalt (Fig. S32)? The Apollo-16-like meteorites range from 4.7 to 6.3% FeO and 1.8–2.7 $\mu\text{g g}^{-1}$ Th, yet only 0.6% of the lunar surface lies within those ranges (Table 5; the analysis of Caldada-Diaz et al. [2015], however, suggests a greater fraction). Perhaps the meteorites originate from only two to three craters, in which case the ejecta were compositionally and texturally diverse. Unfortunately, there are no published cosmic-ray exposure data for any of these stones except NWA 7022 and MIL 090036 (Nishiizumi and Caffee 2013; Fig. S34).

Basaltic Breccias

This section focuses on mafic breccias, those with >12% FeO (Fig. 2) and >25 $\mu\text{g g}^{-1}$ Sc (Fig. 6), that is, those containing greater than about one-third material from the maria. As noted earlier, NWA 6687 (symbol “V” at [41,19] on Fig. 6) is a 42-g (regolith?) breccia that, like the Apollo 12 regolith, is largely a subequal mixture of mare basalt and KREEP-rich material from the PKT with a negligible proportion of FHT material (Figs. S38 and S39 in supporting information). It has the greatest TiO₂ concentration of any of the lunar meteorites for which we have data, 3.9%, thus the basalt component is likely a high-Ti basalt (Fig. S32).

Compositionally, three other basaltic breccias appear to consist almost entirely of brecciated basalt or gabbro. (1) One is the NWA 773 clan discussed below. (2) With 25% FeO, the brecciated portion of dilithologic NEA 003 (Haloda et al. 2006) is the most Fe-rich lunar meteorite that we have studied. It is significantly different in composition from the basalt portion of the meteorite in being 1.2 \times richer in FeO,

Table 5. Comparisons of proportions of lunar-meteorite launch sites by compositional type to data derived from the lunar prospector gamma-ray spectrometer (LP-GRS).

Compositional type	Meteorite launch sites						LP-GRS ^c		
	Range		Min	Max	Min	Max	Bin range		<i>f</i>
	FeO %	Th $\mu\text{g g}^{-1}$	<i>N</i> ^a	<i>N</i> ^a	<i>f</i> ^b %	<i>f</i> ^b %	FeO %	Th ppm	
Feldspathic			(54)	(63)	(50)	(51)			(25)
Typical	2.8–5.4	0.1–0.65	32	38	29.6	30.4	2.5–5.5	0.12–0.7	14.9
Atypical	3.1–6.0	0.14–1.3	16	18	14.8	14.4	3.0–5.5	0.7–1.5	9.6
Apollo-16-like	4.7–6.3	1.8–2.7	6	7	5.6	5.6	4.7–6.3	1.8–2.7	0.6
Troctolitic	3.1–5.7	0.07–0.10	5	6	4.6	4.8	2.5–7.0	0–0.12	4.1
Anorthositic noritic, <0.7 $\mu\text{g g}^{-1}$ Th	5.3–8.6	0.11–0.9	16	17	14.8	13.6	5.5–12.5	0.1–0.7	11.7
Anorthositic noritic, 0.7–3.5 $\mu\text{g g}^{-1}$ Th	5.5–12.7	0.7–3.2	16	20	14.8	16.0	5.5–12.5	0.7–3.5	27.3
Noritic (KREEP), >3.5 $\mu\text{g g}^{-1}$ Th	9.4–16.3	>3.5	6	6	5.6	4.8	7.2–15.9	3.5–12.5	5.4
Basaltic	12.5–21.2	0.4–2.8	4	6	3.7	4.8	12.5–22	0.2–3.5	12.9
Mare basalt	17–23	0.4–2.1	6	6	5.6	4.8			
KREEPy mare	15.9–23	>3.5	1	1	0.9	0.8	15.9–23	>3.5	7.8
Other									
Highly feldspathic	0	0	0	0	0.	0.	0–2.5	0.9–1.9	2.7
Feldspathic, high Th	0	0	0	0	0.	0.	2.5–6.2	0.7–6.1	2.5
Th \leq 0	0	0	0	0	0.	0.	0.9–2.5	0	0.3
							7–12.3		
Sum			108	125	100.	100.			100.

^aBased on 108 of the 109 minimum launch sites of Table 4 for which there are FeO and Th data.

^bBased on 125 of the 134 maximum launch sites of Table 4 for which there are FeO and Th data.

^cBased on the 1° (30 km) derived data from the lunar prospector gamma-ray spectrometer (data of Lawrence et al. [2000] and Prettyman et al. [2006], with calibration of Gillis et al. [2004]). See also Fig. S3b.

~2× richer in incompatible elements, and having different relative concentrations of REE (Figs. S14e and S40 in supporting information). There is no petrographic (Haloda et al. 2006) or compositional evidence for an FHT component in the breccia. Curiously for a breccia, Ni (<200 $\mu\text{g g}^{-1}$) and Ir (<9 ng g^{-1}) concentrations are below our detection limits. Like Dhofar 287 (Demidova et al. 2003) and SaU 169 (Sayh al Uhaymir, Gnos et al. 2004), NEA 003 is essentially a regolith breccia with one large clast of an igneous lithology that is not a dominant lithology in the fine-grained brecciated portion of the rock. (3) NWA 11886 (symbol “I” at [67,21] on Fig. 6) is a 36-g fragmental breccia that also has high concentrations of incompatible elements. It has the greatest Sc concentration (67 $\mu\text{g g}^{-1}$) of any brecciated lunar meteorite that we have studied and a high FeO concentration typical of mare basalt, 21% (point [21,2.7] of Fig. 2). Thus, unlike NWA 6687, the breccia must contain only a negligible proportion of an admixed KREEP component (typically 10–12% FeO and 20–26 $\mu\text{g g}^{-1}$ Sc) because KREEP would effectively dilute the concentrations of both FeO and Sc, which has not occurred. The high incompatible element concentrations in NWA 11886 must be a characteristic of the basalt from which the rock derives and are

comparable only to those of the high-Ti basalts of Apollo 11 (groups A, B1, and B2 of Beatty et al. 1979). No TiO₂ data are available, but the high Sc is consistent with high TiO₂ (Fig. S32). The meteorite is relatively depleted in light REE (Fig. S13f).

Fifteen lunar meteorite stones are breccias that plot near the mare apex of the mixing triangle of Fig. 6 along or near the FHT-mare join at 25–50 $\mu\text{g g}^{-1}$ Sc (Fig. S41 in supporting information). These breccias are largely devoid of a PKT component but likely contain >40% mare material. Eight are from northern Africa, six are from Antarctica, and one is from Oman (Dhofar 1180, the least basaltic of those discussed here; Korotev 2012). On the basis of composition, petrography, and some cosmic-ray exposure data, all six of those from Antarctica (regolith breccias) are either paired or launch paired with each other (Korotev and Zeigler [2014] and sources cited therein; Collareta et al. 2016). Almost certainly, the “YQEND” launch-pair group (Yamato, Queen Alexandra Range, Elephant Moraine, NWA 4884 [1 stone, 48 g], and Mount DeWitt [DEW] 12007) also includes the NWA 7611 clan (7611, 8277, 10480, and 10566; 2.35 kg). None of the stones of the NWA 7611 clan is described as a regolith breccia, however. Except for Ba (high in the NWA 7611 clan), these meteorites are all indistinguishable from each other in

composition and have the uncommon property of increasing Na and Eu concentrations with decreasing Fe and Sc among subsamples (Figs. S41 and S42 in supporting information). All are regolith or fragmental breccias that, compositionally, are subequal mixtures of atypically sodic anorthosite from the FHT and a low-Ti mare basalt (Jolliff et al. 1998; Arai and Warren 1999). Cosmic-ray exposure data allow that DEW 12007, NWA 4884, and NWA 8277 (NWA 7611 clan) are all launch paired (Nishiizumi et al. 2016). NWA 10447 is compositionally most similar to NWA 4884 and the NWA 7611 clan, but there are some clear differences (Fig. S41).

NWA 3136 (symbol “G” at [47,4] on Fig. 6) is compositionally distinct from the other NWA basaltic breccias in being one of the most Sc rich but similarly poor in incompatible elements with a slight HREE enrichment (heavy REE, Fig. S13b). Kuehner et al. (2005) note that most of the lithic clasts are mare basalts, including some high-Ti mare basalts, which do not occur as discrete meteorites, while O'Donnell et al. (2008) did not observe mare basalts or mafic glasses. Both studies, however, observed mafic lithologies like anorthositic norite, gabbroic norite, olivine-bearing norite, and orthopyroxene–olivine-bearing anorthosite. Mg' is 55, at the high end of the range for mare basalts (Fig. 10), so the NWA 3136 breccia is ambiguous in being either, at one extreme, a mare-FHT mixture with moderately magnesian mare component or, at the other extreme, a breccia containing significant proportion of mafic, magnesian, nonmare material.

Although we have not obtained INAA data for NWA 12384, preliminary major element data of Carpenter et al. (2019) suggest that it is a unique brecciated meteorite derived entirely from mare basalt. Concentrations of Al_2O_3 , FeO, and Sc are typical of a mare basalt mixed with minimal FHT material (Figs. 10 and 13d) and the low K_2O concentration (0.01%) indicates negligible KREEP. Like NWA 3136 and the YQEND basaltic breccias, Mg' (55) is at the high end of the range for mare basalts (Fig. 10), suggesting a possible nonmare mafic component. We do not have INAA data for NWA 11524, but the EPMA data for a melt vein in the rock have 18.9% FeO, 11% Al_2O_3 , 3% TiO_2 (C. Agee in MetBull), unlike any other basaltic breccia among lunar meteorites.

Anorthositic-Noritic and Basalt-Bearing Feldspathic Meteorites

In this section, we address the ~22 meteorites, all breccias, with 11–30 $\mu g\ g^{-1}$ Sc and <9 $\mu g\ g^{-1}$ Sm (Fig. 6). Most plot in the anorthositic norite fields of Figs. 6, 8, and 10. At one extreme are basalt-bearing

(10–40% basalt) feldspathic breccias like those discussed in the previous section. At the other extreme are moderately mafic breccias with a substantial nonmare component. The distinction cannot be made unambiguously from bulk composition and few of the meteorites have been studied in detail petrographically. Most of these meteorites, however, show geochemical evidence of having a greater abundance of high- Mg' mafic phases than any reasonable mixture of material from the FHT and mare basalt (Fig. 14; Figs. S4, S5, S43 and S44 in supporting information).

Low-Sc, Sm-Poor “Anorthositic Norites”

Half of the anorthositic-norite breccias are poor in incompatible elements (<2 $\mu g\ g^{-1}$ Sm; Fig. S45 in supporting information). The best characterized is the NWA 3163 clan (Irving et al. 2006; Hudgins et al. 2011a; McLeod et al. 2016). The rocks (four stones, 2.45 kg) are ferroan granulitic breccias of anorthositic norite mineralogy (mean normative mineralogy for NWA 3163 and NWA 4881: 73 wt% plagioclase, 16 wt% hypersthene, 6 wt% diopside, 3.5 wt% olivine, and 0.4 wt% ilmenite) with $Mg' = 62$, a low value for a nonmare rock but greater than that of any mare basalt (Fig. 10). No mare basalt clasts are reported. Hudgins et al. (2011a) obtained a ^{39}Ar - ^{40}Ar age of 3327 ± 29 Ma for NWA 3163 and associated the age with a high-temperature metamorphic event. Hudgins et al. (2011b) concluded that the meteorite and similar Apollo samples that they studied “formed above or beneath superheated impact melt sheets associated with medium-size (100–200 km) craters.” The moderately mafic mineralogy and low concentrations of incompatible elements (Fig. S45) suggest a deep crustal origin in the FHT at a point distant from the PKT, but also distant from the source region of the troctolitic NWA 5744 clan (Fig. S45).

Similarly, there is no compositional or petrographic evidence that NWA 4932 ($Mg' = 66$), the most mafic of the breccias of Fig. S45 (8.6% FeO, 20 $\mu g\ g^{-1}$ Sc), contains mare basalt (Korotev et al. 2009). In the subsample data cluster, there is no significant variation in Sc concentration, that is, there is no evidence of feldspathic or mare-basalt clasts, and Sm/Th is less than that of mare basalts (Fig. S45b,d). The rock is a metal-rich (Fig. S1b) impact-melt breccia “composed of small gabbroic to troctolitic clasts” (Irving and Kuehner, MetBull) that likely formed from moderately mafic nonmare material. Normatively, the rock is 61% plagioclase ($An_{96.6}$), 5% diopside, 22% hypersthene, 10% olivine, 0.7% ilmenite, and $Mg' = 66$.

Compositionally, NWA 10986 (NWA 10509 clan) is a low-Sm (0.9 $\mu g\ g^{-1}$) anorthositic norite (Roberts et al. 2019). In addition to low-Ti and very-low-Ti basalts, it contains a variety of moderately mafic, unbrecciated,

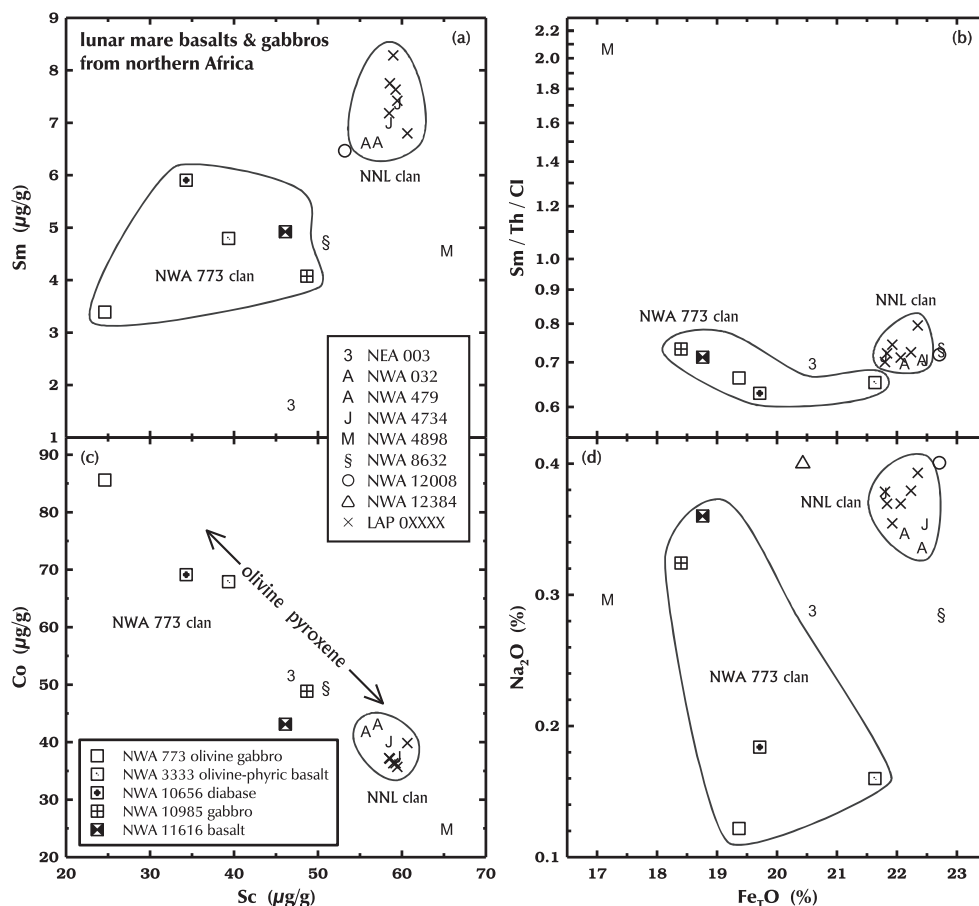


Fig. 13. Data for mare basalts among lunar meteorites from northern Africa (stone means). a–d) The NNL launch-pair group (NWA 032/479, NWA 4734/10597, and LAP plus and 5 pairs) cluster tightly. NWA 8632 may be an olivine-rich launch pair of the NNL clan; see text. a, b, d) NWA 12008 (data of Cohen et al. 2019) is very similar to the NNL clan, but it has a different texture. b) NWA 4898 has distinctly high Sm/Th. c) There are no Co data for NWA 12008. d) NWA 12384, the only breccia plotted here (data of Carpenter et al. 2019), has an FeO concentration typical of mare basalt, indicating that there is only a minor component of nonmare material. On the basis of major element data alone, there is no evidence that NWA 12384 is paired with another NWA basalt.

nonmare clasts including troctolite, anorthositic norite, and gabbro-norite. On the basis of the model of Fig. 6, the mare component is at most 15%.

Some of the other meteorites of similar composition (Fig. S45) are more mafic than typical feldspathic meteorites because they contain minor amounts of mare basalt. Basalt clasts (sparse) are reported in the MetBull descriptions of NEA 001, NWA 8055, NWA 10626, and NWA 10798. INAA data for NEA 001, NWA 8055, NWA 10495, and NWA 10626 are consistent with a minor component of mare basalt but those for the NWA 10509 clan, NWA 11127, and Rabt Sbayta 008 are ambiguous (Fig. S45).

Moderately High-Sm “Anorthositic Norites”

The other half of the anorthositic-mafic breccias have moderately high concentrations of incompatible elements, 2–8 μg g^{−1} Sm (0.8–3.1 μg g^{−1} Th, Fig. S3),

that is, less than that of the Apollo-16-like meteorites and equivalent to ~1% (NWA 8673 clan) to 18% (NWA 8182) KREEP component of Fig. 6 (Fig. S46 in supporting information). Normative plagioclase ranges from 47 to 70 wt% (~55–75 vol%) among those for which there are major element data, that is, most plot in the anorthositic norite field of Fig. 8.

The best characterized is the NWA 2995 clan (11 stones, 2.22 kg, 48–59% normative plagioclase; Fig. S47 in supporting information). Korotev et al. (2009) report “clasts of anorthosite, anorthositic norite, anorthositic troctolite, norite, troctolite, gabbro, granulitic breccia, mare basalt, and glass of KREEP-basalt composition” in several stones of the NWA 2995 clan. In NWA 2996, Mercer et al. (2013) observe “The most prominent clast lithologies are noritic and troctolitic anorthosites, gabbro and peridotite, and a disaggregated evolved lithology comprised of ferroan pyroxenites, Na-rich plagioclase

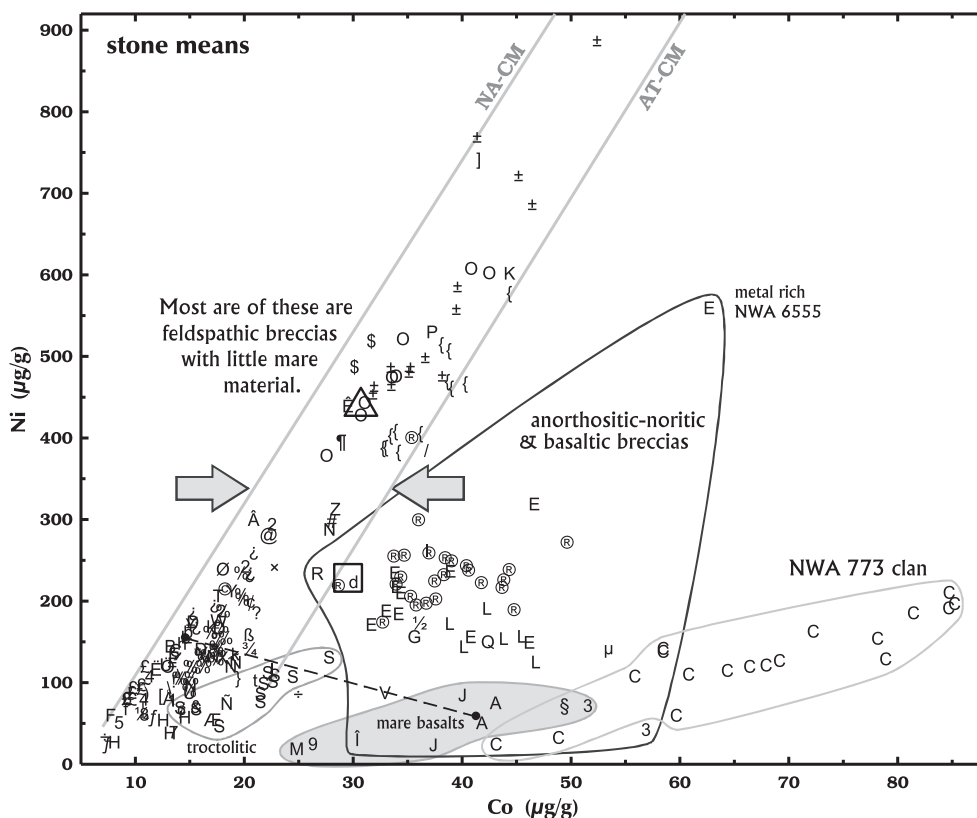


Fig. 14. Lunar meteorites from northern Africa in Co-Ni space. The solid diagonal lines are mixing lines between feldspathic meteorites of noritic anorthosite (NA, lower Co) and anorthositic troctolite (AT, higher Co) composition and CM chondrites. Most feldspathic lunar meteorites lie between the two lines, that is, their Ni and Co concentrations are largely consistent with mixtures of nonmare pyroxene, nonmare olivine, and chondritic material. The olivine-rich (troctolitic) meteorites have greater concentrations of indigenous Co. Unbrecciated mare basalts have high Co and low Ni. High-Co brecciated meteorites plotting outside the diagonal lines are anorthositic-noritic and basalt-bearing breccias. (The olivine-rich NWA 773 clan consists of basalts, gabbros, and breccias.) For anorthositic-noritic and basalt-bearing breccias (NWA 2995 clan [E], NWA 3136 [G], NWA 5153 [Q], NWA 6687 [V], NWA 7611 clan [L], NWA 7834 clan [®], NWA 8182 [½], NWA 10447 [μ], NWA 11886 [I], and the NEA 003 breccia [3]), Co and Ni are largely associated with nonmare lunar olivine, not with meteorites (Figs. 12; Fig. S49e) or mare basalt; the dashed diagonal line is the FHT-mare mixing line of the mixing triangles of Figs. 2 and 6; few high-Co meteorites plot along this line. For reference, the large triangle represents the mean composition of typical Apollo 16 soils and the large square represents the Luna 20 soil. Symbol key in Table S1.

fragments, and granophyric alkali feldspar and silica clasts Impactites are less abundant, and include anorthositic granulitic breccias, granulites, and glassy melt breccias Clasts of basalt are rare.” For the five stones for which we have major element data, Mg' ranges from 56 to 60, that is, greater than any likely mixture of FHT material and mare basalt (Fig. 10; Fig. S46). Plagioclase in the NWA 2995 clan is more sodic than is typical of feldspathic lunar meteorites (Fig. S47b,c). Thus, the NWA 2995 clan represents a moderately mafic region of nonmare crust. The same is largely true of NWA 4819 (62% normative plagioclase and $Mg' = 66$), NWA 5153 (49% and 55), NWA 5207 (67% and 62), NWA 6888 (76% and 60), the NWA 7834 clan ($57 \pm 9\%$ and 60), the NWA 8673 clan ($\sim 64\%$), and NWA 11243 ($\sim 73\%$; Fig. S46S).

Normatively, the large (25 stones totaling 21 kg) NWA 7834 clan varies considerably in olivine/pyroxene and is less sodic than the NWA 2995 clan (Figs. S48 and S49 in supporting information). Again, the composition is largely not consistent with any mixture of typical material of the FHT and mare basalt (Fig. S46a,c). Lithic clasts reported in stones of the NWA 7834 clan include anorthosite, anorthositic gabbro, gabbroic anorthosite, anorthositic troctolite, gabbro, troctolite, ultramafic clasts, granulite, impact melt breccia, VLT basalt, evolved basaltic clasts, quartz monzodiorite, and symplectites (Boyle et al. 2018; Stephant et al. 2019; Zeng et al. 2019).

For the 13 stones of the NWA 8673 clan (12.3 kg), clasts of mare basalt are rare and Cr/Sc is greater than any FHT-mare mixture (Fig. S46), but no mafic

nonmare lithic clasts are reported in the MetBull descriptions. On the basis of bulk composition and high metal content, the NWA 8673 clan may be launch paired with the Dhofar 925 clan and Sayh al Uhaymir 449 from Oman (Fig. S50 in supporting information). Of the potential launch-pair stones for which we have major element data, NWA 7274 (69% normative plagioclase) has the greatest Mg' (70) but no mafic clasts are reported in the MetBull description.

If we have lunar meteorites from the South Pole–Aiken basin, and the probability is high that we have several (Korotev et al. 2009), then they are likely to occur among the meteorites discussed in this section. Some of these meteorites, most notably the NWA 8673 clan and, to a lesser extent the NWA 7834 clan, have compositions that largely (Figs. S49 and S50), but not entirely (Fig. 14; Fig. S6), overlap with soil from the Luna 20 mission, which is largely ejecta from Mare Crisium (Figs. S49 and S50 in supporting information) and likely contains material from the lower crust or upper mantle (Wieczorek et al. 2006).

Unbrecciated Mare Basalts and the NWA 773 Clan

We provide new compositional data for mare basalts NEA (Northeast Africa) 003, NWA 479, NWA 4734, NWA 4898, and NWA 8632, as well the basaltic lithologies in breccias NWA 10597 and NWA 11616 of the NWA 773 clan (Tables S2–S4).

Dilithologic NEA 003 (124 g; 3089 ± 64 Ma, Haloda et al. 2009; Sm–Nd) is a breccia dominated (~75%) by a large clast of low-Ti basalt (Fig. S51 in supporting information; Haloda et al. 2009). The basalt has the lowest concentrations of REE (Fig. 13; Fig. S52 in supporting information) and, except for the NWA 773 clan, which contains cumulate olivine, the highest Mg' (64) of the basalts studied here (Fig. 10).

NWA 4898 (137 g; 3578 ± 59 Ma; Gaffney et al. 2008; Rb–Sr) is distinct in being the only high-alumina (11.8% Al_2O_3 , Table S4) basalt among lunar meteorites (Greshake et al. 2008). Li et al. (2016) note that mineral and bulk chemical compositions of NWA 4898 are more similar to the high-Al basalts of Apollo 14 (typically, 12.0–12.5% Al_2O_3) than to the aluminous basalts of Luna 16 (13.5% Al_2O_3) and Apollo 12 (sample 12038, 13.0% Al_2O_3). Among the African lunar basalts, NWA 4898 has the lowest La/Sm (“light REE depletion,” Fig. S14).

NWA 032 (300 g) and its pair NWA 479 (156 g; Fig. S51) are well-studied low-Ti basalts (Fagan et al. 2002; Fernandes et al. 2003, 2009; Day and Taylor 2007; Borg et al. 2009; Elardo et al. 2013) with a “young” crystallization age of 2947 ± 16 Ma (Borg et al. 2009; Rb–Sr). Subsamples of the two stones overlap in

composition for all elements determined (Fig. S52). NWA 4734 (1.37 kg; 3024 ± 27 Ma; Elardo et al. 2013; Sm–Nd) and its pair NWA 10597 (350 g) are low-Ti basalts (Figs. S51 and S52; Chen et al. 2019b) that are launch-paired with the six LaPaz Icefield basalts from Antarctica (Zeigler et al. 2005). Despite some minor compositional differences (Fig. S52), Korotev and Zeigler (2014) suggest that NWA 032 is also launch paired with NWA 4734 and the LAP meteorite and together form the “NNL” launch-pair group. $^{147}Sm/^{144}Nd$ data indicate that NWA 032 and the NWA 4724-LAP pair are “derived from similar, but distinct, source materials” (Elardo et al. 2013), but the data do not rule out the launch-pair hypothesis. Preliminary compositional data for NWA 12008 (577 g) suggest that the rock is nearly identical in composition to NWA 032/479 and NWA 4734/10597 (Fig. 13; Cohen et al. 2019). The crystal size distribution of plagioclase in NWA 12008 is similar to that of the LAP meteorite (Webb et al. 2019), yet the textures are different (Cohen et al. 2019). Finally, preliminary compositional data for diabase NWA 12839 (69 g; Burney et al. 2020) is also largely indistinguishable from data for the NNL stones, yet, again, the diabasic texture is distinct. If NWA 12008 and NWA 12839 have low crystallization ages like that of the NNL clan, then it is possible that a single, perhaps moderately large, impact on the Moon launched at least five texturally diverse rocks that made their way to Earth. Nishiizumi (2003) estimates an ejection age of $46 \pm 7 \times 10^4$ years for NWA 032.

Small (24 g) NWA 8632 is a porphyritic, low-Ti basalt (Korotev et al. 2015; Cato et al. 2016; Fagan et al. 2018a; Tang et al. 2018). Several studies note petrologic similarities to NWA 032 (Fagan et al. 2018a, 2018b; Webb et al. 2019). $^{40}Ar/^{39}Ar$ geochronology yields indistinguishable crystallization ages: 2772 ± 41 Ma and 2877 ± 34 Ma for NWA 8632 (2 aliquots; Fagan et al. 2018a) and 2779 ± 14 Ma for NWA 032 (Fernandes et al. 2003). Major element concentrations are most similar to those of Apollo 12 pigeonite and olivine basalts as well as NWA 032 (Fig. S51). In detail, compared to NWA 032, concentrations of incompatible elements are $0.7\times$ lower (Fig. S52a) and Cr/Sc is higher (66 versus 49; Fig. S52d) in NWA 8632. The major element composition of NWA 8632 is matched reasonably well, however, by 83% NWA 032, 13% Fo₆₈ olivine, and 3% ilmenite, which permits the suggestions that (1) NWA 8632 is a sample from the bottom of the NNL basalt flow, one that contains denser minerals and slightly less trapped liquid than NWA 032, and (2) NWA 8632 is a sixth member of the NNL launch pair group.

Despite reported find locations that are as great as 1160 km apart (NWA 773 and Anoual, MetBull), the

NWA 773 clan (11.9 kg) consists of 16 stones that apparently all represent a fragmental or regolith breccia containing large (up to at least 10 cm) clasts of basaltic and gabbroic lithologies, some to all of which are genetically related (Fagan et al. 2003; Jolliff et al. 2003; Zeigler et al. 2007; North-Valencia et al. 2014; Nagaoka et al. 2015; Shaulis et al. 2017; Valencia et al. 2019). On the basis of 50 baddeleyite grains from four of the NWA 773 clan stones, Shaulis et al. (2017) report a weighted mean ^{207}Pb - ^{206}Pb crystallization age of 3115.6 ± 6.8 Ma for the clan. The breccia is all but devoid of FHT material. Among the 12 stones studied by Valencia et al. (2019), olivine-phyric basalt occurs in four stones, olivine gabbro in ten stones, ferroan gabbro in five stones, anorthositic gabbro in three stones, and fragmental breccia in seven stones. Valencia et al. (2019) reason that all four igneous lithologies are products of a single igneous system. A characteristic of the NWA 773 clan igneous rocks is low concentrations of Na and Eu compared to other mare basalts ($\sim 0.5\times$; Figs. S5, S52, and S16).

Since the work of Valencia et al. (2019), more recently discovered NWA 11616 (2.55 kg) consists of breccia that is compositionally identical to the NWA 773 clan breccias. It hosts a large clast of olivine-free basalt, however, that is distinctly more sodic than any of the previously studied igneous clasts of the NWA 773 clan (Fig. S53 in supporting information) and has different relative concentrations of REE (Fig. S14f). A large clast (at least 4 cm) in NWA 10985 (250 g, gabbro) is similar (Figs. S14f and S53). It has not been established whether or not the sodic gabbro is genetically related to the other NWA 773 clan igneous lithologies. There are no major element or geochronologic data but trace element data do not suggest a genetic relationship (Figs. S14f and S53; Chen et al. 2019a).

Another olivine gabbro, NWA 12393 (1.27 kg), is not self-evidently related to the NWA 773 clan in that the olivine is more forsteritic and the plagioclase is more anorthitic (Table S2). Similarly, gabbro Swayyah 001 (4.6 kg) is coarser grained than the NWA 773 clan and much more ferroan ($Mg' = 48$; Shi et al. 2020) than the olivine gabbro of the NWA 773 clan (Fo_{60-70} , En_{60-80} ; Valencia et al. 2019). These two rocks need more study.

Ignoring small clasts of mare basalt that occur in many lunar meteorites, 6–10 locations on the Moon are represented by unbrecciated basalts among the lunar meteorites, including (1) Dhofar 287 from Oman, (2) the YAM launch pairs from Antarctica (Yamato 793169, Asuka 881757, and Miller Range 05023), (3) NEA 003, (4) the NNL launch pairs (NWA 032/479, NWA 4734/10597, the LaPaz Icefield stones and,

possibly, NWA 8632 and NWA 12008), (5) NWA 4898, (6) those igneous lithologies of the NWA 773 discussed by Valencia et al. (2019), and (7–10) tentatively pending comprehensive study, (7) the sodic, olivine-poor basalts of NWA 11616 and NWA 10985 (NWA 773 clan), (8) NWA 12393 (olivine gabbro), (9) NWA 12839 (diabase), and (10) Swayyah 001 (gabbro). For the mixing triangles of Figs. 2, 6, and 10, the mare apices are represented by the mean composition of the meteorites of the first six of the assumed launch sites (Fig. S4).

Nickel, Cobalt, Iridium, and Gold in Brecciated Meteorites

Nearly all brecciated lunar meteorites contain detectable concentrations of Ir at levels $>1 \text{ ng g}^{-1}$ (Fig. 12). Several of the basaltic breccias have concentrations of Ir below our rather high detection limits for basaltic compositions (Fig. 12): $<7 \text{ ng g}^{-1}$ for NWA 773 clan, $<12 \text{ ng g}^{-1}$ for NEA 003, and $<12 \text{ ng g}^{-1}$ for NWA 6687. Among the feldspathic breccias, however, the lowest Ir concentrations are observed in Rabt Sbayta 008 ($0.7 \pm 0.3 \text{ ng g}^{-1}$, clast-rich leucocratic), NWA 11182 ($1.4 \pm 0.6 \text{ ng g}^{-1}$, fragmental), the NWA 3163 clan ($1.7 \pm 0.6 \text{ ng g}^{-1}$, ferroan granulitic), the NWA 5744 clan ($1.7 \pm 0.3 \text{ ng g}^{-1}$, magnesian granulitic), and NWA 10495 ($1.8 \pm 0.6 \text{ ng g}^{-1}$; fine-grained fragmental). These low Ir concentrations are equivalent to 0.1–0.3% CM chondrite (Fig. 12).

More typically, particularly in meteorites that are regolith breccias, Ir concentrations are equivalent to 0.5–1.7% CM chondrite (Fig. 12; Fig. S36). The mean Ir concentration of the typical feldspathic meteorites is 6.5 ng g^{-1} , equivalent to 1.1% CM chondrite (Fig. 12). In most low-Ir breccias, Ir concentrations are rather constant and normally distributed among subsamples, as we would expect if the Ir derives mostly from chondritic micrometeorites (Fig. 15a). In contrast, for lunar meteorites with high abundances of siderophile elements, concentrations are not normally distributed among subsamples because a portion of the siderophile elements is carried by grains of FeNi metal (Fig. S36). Metal grains greater than a millimeter in diameter occur in NWA 5000 (e.g., Fig. S28) and we have seen a photograph of slice of NWA 8666 (NWA 8455 clan) containing a 3 mm metal grain. We have calculated siderophile element ratios and estimated concentrations of Ni, Ir, and Au in the metal of several metal-rich meteorites (Table S6; Fig. S54 in supporting information). Ni/Co, Ir/Co, and Ir/Ni are usually lower in metal from metal-rich lunar meteorites than in metal from ordinary chondrites but are in the range of iron meteorites (Fig. 15b; Fig. S55 in supporting

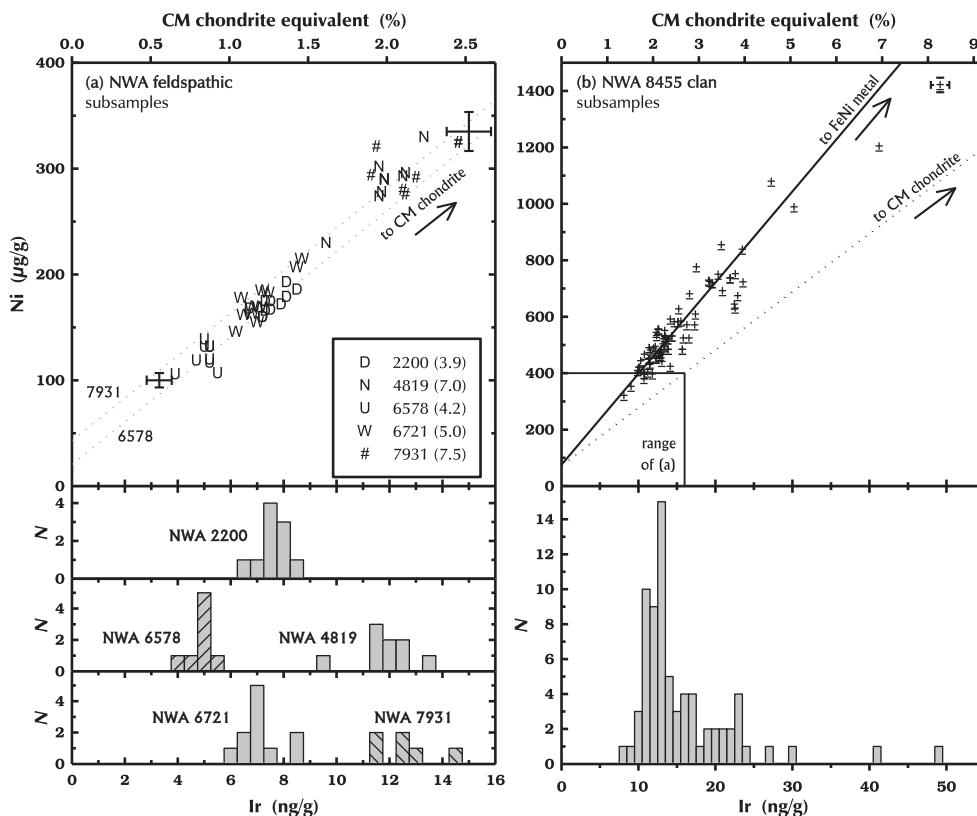


Fig. 15. a) Lunar meteorites of this plot are all feldspathic (% FeO_T concentrations in parentheses in legend) and have the property that concentrations of Ni and Ir are rather constant and, perhaps, normally distributed among subsamples because the carrier of Ni and Ir is fine-grained and uniformly dispersed. This condition occurs, for example, in regolith breccias where CM micrometeorites are the main source of the two elements (Wasson et al. 1975), not nuggets of FeNi metal (Fig. 12). For reference, the dashed lines are defined by the mean concentrations of Ir and Ni in the NWA 6578 subsamples (low FeO_T) or NWA 7931 (high FeO_T) and CM chondrites ($\text{Ni}/\text{Ir} = 2.1 \times 10^4$; Lodders and Fegley 1998). The Ni intercepts (zero Ir) represent the Ni carried by mafic minerals and presumably are greater in NWA 7931 than in NWA 6578 because the mafic-mineral (and FeO_T) concentration is greater in the former. The error bars represent typical 1- σ analytical uncertainties at the two ends of the trend. b) In contrast, in other meteorites such as the NWA 8455 clan, Ni and Ir concentrations are greater, on average, than in the meteorites of (a), highly variable, and not normally distributed. For such meteorites, there may be a micrometeorite component, but siderophile elements are carried in part by FeNi metal grains; Ir-rich subsamples contain larger or more grains. Ni/Ir ratios in the metal-rich meteorites are usually inconsistent with ordinary and carbonaceous chondrites but are consistent with some classes of enstatite chondrites and iron meteorites (Fig. S55; Table S6).

information). When data for the entire suite of siderophile elements are considered, as for NWA 5000 (Humayun and Irving 2008), the metal composition may not be an exact match to any known type of meteorite.

Gold concentrations in NWA lunar meteorites are sometimes anomalously high from terrestrial contamination and we have observed at least one case where gold has been lost due to terrestrial weathering effects (Fig. S56 in supporting information; cf. Wasson 2019).

How Many Lunar Meteorites and Launch Sites?

We estimate (in supporting information) that the 341 characterized lunar meteorite stones (86% of the total) represent about 140 (uncertainty range: 131–147)

meteorites (and meteoroids) when likely terrestrially pairings are considered (Table 4; Table S7). This estimate is an upper limit if there are more terrestrial pairings than we recognize on the basis of composition. The estimate leads to an average of 2.4 stones/meteoroid, although among individual meteorites the ratio ranges from 1 (e.g., NWA 5000) to 40+ (NWA 8046).

In turn, as result of launch pairings (e.g., NWA 4734 and the LaPaz Icefield basalts of Antarctica), we estimate that the 131–147 meteorites originate from 109 to 134 launch sites on the Moon (Table 4; Table S7). The lower limit ($N = 109$) is the estimated minimum number of meteorites ($N = 131$) minus the number of meteorites (22) that are “likely” (13) and “possible” (9) launch pairs of the 10 launch-pair groups

of Table 4 and Table S7. The upper limit is the estimated maximum number of meteorites ($N = 147$) minus those meteorites (13) that are “likely” launch pairs (i.e., the “possible” launch pairs may, in fact, not be paired, so count all of these stones as representing launch sites for the “maximum” estimate). For convenience, we will use the mean and range, 122 ± 12 , for purposes of discussion. The mean is equivalent to about one crater per $3.1 \pm 0.3 \times 10^5 \text{ km}^2$, an area about the size of Belgium or the state of Maryland. We acknowledge that these estimates are based mainly on the assumptions that (if consistent with available petrography and cosmic-ray exposure data, e.g., Nishiizumi 2003) demonstrably different compositions indicate different meteorites (no terrestrial pairing) and that demonstrably similar compositions at different geographical locations suggest launch pairing. We recognize (as did a reviewer) that 140 meteorites from as many as 122 sites on the Moon leads to a ratio of 1.15 meteorites/site, much lower than for Mars where the ratio is at least 20. Our launch-site estimate for lunar meteoroids cannot be significantly lower than 109, however, without making many arbitrary and unsupportable “lumpings.”

Comparison to Orbital Gamma-Ray Data

Among the lunar-meteorite launch sites (minimum estimate of Tables 4 and 5), 50% are feldspathic with 2.8–6.3% FeO and $0.1\text{--}2.7 \mu\text{g g}^{-1}$ Th (first three rows of Table 5). This value compares with 25%, half as great, of the lunar surface with the same FeO and Th concentration ranges as derived from the LP-GRS data (Lunar Prospector gamma-ray spectrometer; Table 5 and Fig. S3b). The discrepancy suggests that there are more terrestrial or launch pairings among the 54 meteorites of this compositional type than we identify. In order to decrease the proportion of feldspathic launch sites from 50% to 25%, we must assume that we have overestimated the number of feldspathic launch sites by a factor of 3.0, decreasing the number of launch sites from 54 to 18. The ratio of total meteorites to launch sites (among those that have compositional data), however, increases from 1.15 to only 2.0, still very much lower than the Martian value (>20). We do not know the cause of this discrepancy between the feldspathic meteorites and the LP-GRS data. We suspect that for this comparison, Mars is not a good analog of the Moon, however, because the Moon has 0.4 times the gravity of Mars and is much closer to Earth.

For the Apollo-16-like composition, 5.6% of the launch sites are in the compositional range of Apollo 16 soil but only 0.6% of the lunar surface (Table 5). As

noted above, the discrepancy suggests that there may be unrecognized pairings among the six launch pairs that we identify of this composition. To lower the number of launch sites from 5.5% to 0.6% requires 0.7 meteorites or, effectively, 1. That one meteorite impact on the Moon could have yielded rocks with the divergent compositions of Fig. S35 is doubtful, however, in that the compositional diversity of the meteorites is greater than that of KREEP-bearing breccias from the Apollo 16 site (Korotev 1994).

Lunar meteorites that are troctolitic have low to moderate FeO and very low Th. Five percent of the launch sites and 4% of the surface have these characteristics. The agreement is also good for low-Th anorthositic norite breccias: 15% of the meteorite launch sites and 12% of the lunar surface. The agreement is poorer for the moderate-Th ($0.7\text{--}3.5 \mu\text{g g}^{-1}$) anorthositic norite breccias: 15% of the launch sites compared with 27% of the lunar surface. Most surface of this composition occurs within the inner South Pole–Aiken basin and as distal ejecta of the Imbrium basin (Gillis et al. 2004). The LP-GRS data cannot distinguish between mare basalt and basaltic breccia; all basaltic (high-FeO) surface material observed by the LP-GRS is regolith. The sum of basaltic breccias and mare basalts among the proposed meteorite launch sites, 10%, agrees reasonably well with that proportion of the lunar surface, 13%, with $>12.5\%$ FeO and $<3.5 \mu\text{g g}^{-1}$ Th. Only one meteorite (0.8%), breccia NWA 6687, lies in the “KREEP + basalt” field (high Th plus high FeO) of Fig. S3b, yet 8% of the lunar surface has this composition. All of this basaltic surface material occurs in the western Procellarum area.

Ninety-four percent of the lunar surface as mapped by the LP-GRS lies within the bin ranges corresponding to lunar meteorites of Table 5 and Fig. S3b. The remaining 5.6% is unlike any meteorite in being (1) highly feldspathic ($<2.5\%$ FeO), (2) feldspathic but moderately to highly rich in Th ($0.7\text{--}6 \mu\text{g g}^{-1}$), or (3) having undetectable Th ($<0.1 \text{ ppm}$) but outside the range of troctolitic meteorites with respect to FeO (Table 5). Some of the very low-Th regions may represent troctolite, nevertheless.

Overall, the concordance between the lunar meteorite launch-crater compositions and LP-GRS derived data is not ideal but may reflect imperfect geographical randomness of impacts on the Moon that launched the meteorites (Morota et al. 2005; Le Feuvre and Wieczorek 2008; Gallant et al. 2009).

Terrestrial Weathering Effects

Chemical weathering effects in meteorites from the Sahara are well documented (Crozaz et al. [2003] and

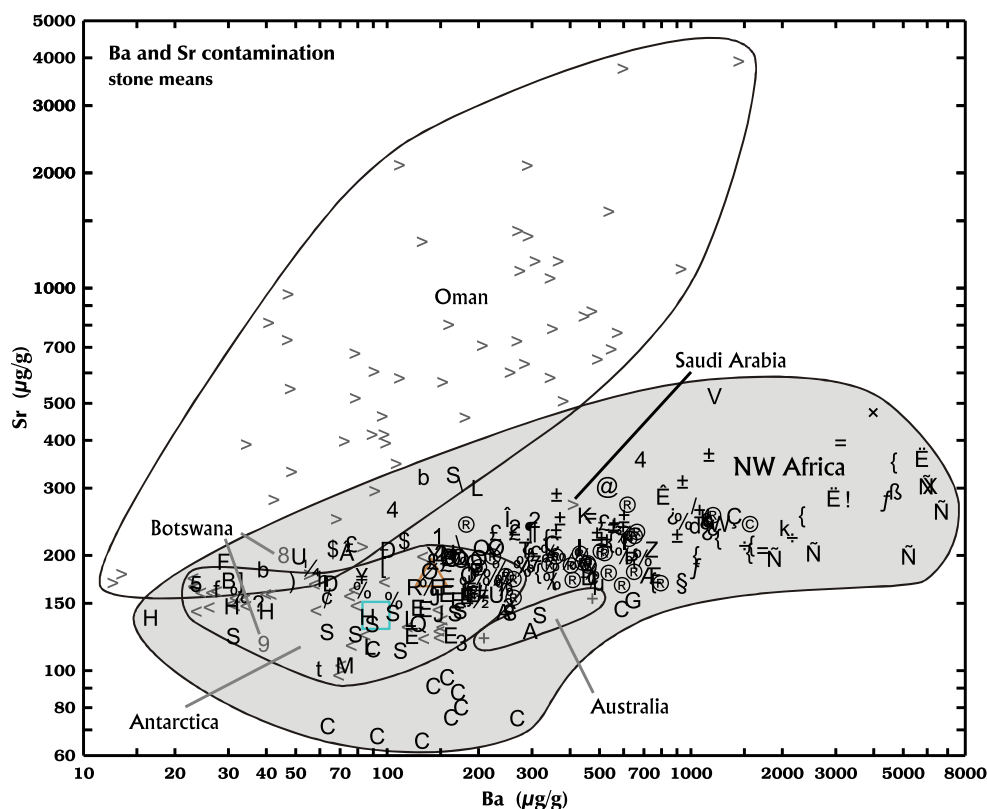


Fig. 16. Stone means in Ba-Sr space and comparison to non-African lunar meteorites. Meteorites from Antarctica are not contaminated with terrestrial Sr or Ba. Note that the symbols for Apollo 16 regolith (obscured large triangle at $140 \mu\text{g g}^{-1}$ Ba) and Luna 20 regolith (large square at $100 \mu\text{g g}^{-1}$ Ba) plot in the Antarctic field. Nearly all lunar meteorites from Oman are enriched in Sr and, to a lesser extent, Ba from terrestrial alteration processes (Korotev 2012). In contrast, many from northern Africa are heavily enriched in Ba. See Table S1 for symbol key for African meteorites. It is largely possible to distinguish an Omani lunar meteorite from a northern Africa lunar meteorite simply on the basis of concentrations of Sr and Ba. (Color figure can be viewed at wileyonlinelibrary.com.)

references cited therein; Korotev 2012). DaG 262, for example, has a terrestrial age of about 80 ± 10 kyr (Nishiizumi 2003) yet as recently as 6 kyr ago northern Africa was tropical to semitropical (e.g., Foley et al. 2003). Our sample of NEA 001 contains a large vein of calcite and gypsum (Fig. S57 in supporting information; Table S2). As noted above, NWA 6721 is likely contaminated with terrestrial Na (brine?). Nearly all African meteorites other than fresh falls (which do not include any lunar specimens) contain small amounts of terrestrial barite, which is readily identifiable by electron microprobe imaging and EDS analysis, whereas most Omani lunar meteorites contain terrestrial celestine and gypsum. Ba and, to a lesser extent, Sr enrichment is a characteristic of meteorites from northern Africa (Bischoff et al. 1998; Crozaz and Wadhwa 2001; Crozaz et al. 2003; Korotev et al. 2003). At the extreme, NWA 6888 (208 g, $6100 \mu\text{g g}^{-1}$ Ba) has $80\times$ its preterrestrial concentration ($\sim 75 \mu\text{g g}^{-1}$ of Ba; Fig. 16; Fig. S67 in supporting information). For feldspathic meteorites with low concentrations of incompatible elements, severalfold

enrichments in K, P, and U occur (Figs. S58 and S59a in supporting information). Relative enrichment in light REE compared to heavy REE is also common (Figs. S7 and S60 in supporting information). In Apollo samples, concentrations of As and Br are below our detection limits but are up to $5.8 \pm 0.8 \mu\text{g g}^{-1}$ As in NWA 11243 and 2.3 ± 0.3 and $6.4 \pm 0.7 \mu\text{g g}^{-1}$ Br in paired stones NWA 4472 and NWA 4485 (Fig. S61 in supporting information). The Br may derive from oceanic aerosols. Among 20 subsamples of NWA 8701 (72 g), arsenic concentrations vary by a factor 8.4, reach $4.5 \mu\text{g g}^{-1}$ in one subsample, and (curiously) correlate positively ($R^2 = 0.92$) with Sc concentration (Fig. S62 in supporting information). A characteristic of all these enrichments is that the magnitude of the contamination varies greatly among subsamples of any given meteorite, for example, Figs. S22e,f, S59b, and S60.

A chemical weathering effect that we have not previously observed or recognized leads to distinct negative Ce anomalies in some NWA meteorites (Fig. 17). Values of Ce/Ce^* (Fig. S63 in supporting

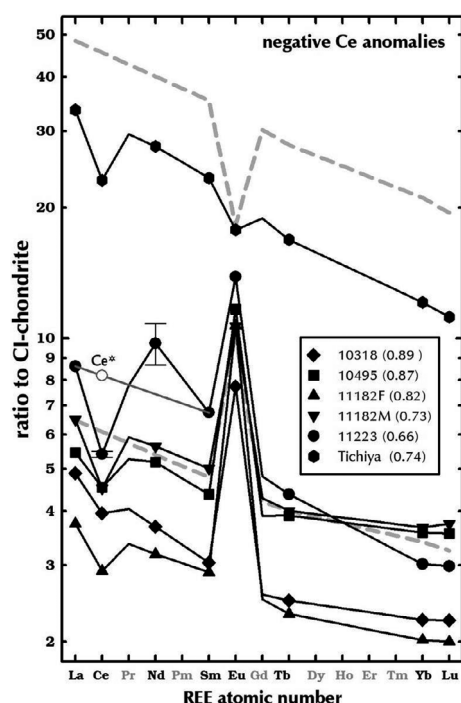


Fig. 17. NWA lunar meteorites with significant negative Ce anomalies. Analyzed REE are those in bold on the abscissa; values for others are interpolated. Nd is the least precisely determined element; 1- σ error bars for Nd (and Ce) are shown for NWA 11223. In the legend, values of Ce/Ce* are given in parentheses, where Ce* is calculated as in Fig. S63 and depicted here for NWA 11223 by the open circle. (Not plotted: NWA 11223 pair NWA 11809 with Ce/Ce* = 0.70.) Two patterns are plotted for NWA 11182 (Fig. S1h), one for the three feldspathic matrix subsamples (F) and the other for the five subsamples of a mafic clast (M). For reference, dashed lines represent mean REE concentrations in typical feldspathic meteorites (bottom) and the Apollo-16-like meteorites (top). Note that compared to these reference patterns, there is little evidence here that the Ce anomalies occur because the trivalent light REE (La, Nd, Sm) are enriched by some weathering effect. However, all of these meteorites have anomalously high Sm/Th (Fig. S15), suggesting that Sm has been enriched by some terrestrial process. See also Fig. 19 and Fig. S63.

information) are as low as 0.66 and 0.70 in paired stones NWA 11223 and 11809 (Figs. 17, S9k, and S63). Among the 11 stones with the deepest negative Ce anomalies, 7 have $>1500 \mu\text{g g}^{-1}$ Ba (Fig. 16), but 16 others with $>1500 \mu\text{g g}^{-1}$ Ba do not have negative Ce anomalies. Four of the 11 (NWA 10318 [CI-normalized La/Sm = 1.6], NWA 11266 [1.7], NWA 11460 [2.0], and Tichiya [1.4]) have La/Sm above the range Antarctic lunar meteorites (1.30–1.37; Fig. S7), so the whole-rock negative Ce anomalies are likely caused by enrichment in trivalent light REE. NWA 11223/11809 and Tichiya are also enriched in Eu, which is divalent on the Moon (Fig. S6). Both the matrix of NWA 11182 and a clast of distinctly different composition (Fig. 17; Fig. S1h) have

Ce anomalies, indicating that the cause of the anomalies is not a lunar process (Qin et al. 2020).

A few meteorites have small positive Ce anomalies (Fig. S63); the effect is most evident in Na-contaminated NWA 6721 (Fig. S9d), which has normal La/Sm (obscured, but at 1.37 in Fig. S7). The latter feature differs from that of Lynch 002 discussed below. Small positive Ce anomalies have also been observed in some lunar meteorites from Antarctica (Ce/Ce*: 1.00–1.03, Kagi and Takahashi 2008; 1.03–1.14, Jolliff et al. 1991).

Comparisons to Some Lunar Meteorites from Botswana, Antarctica, and Australia

Kalahari 008 and 009 Redux

Sokol et al. (2008) identify lunar meteorite Kalahari 009 (13.5 kg) as “a monomict breccia with basaltic composition and mineralogy.” The protolith is a “VLT (very-low-Ti) mare basalt with extremely low contents of incompatible elements” (Sokol et al. 2008). The basalt is one of the oldest known from the Moon (Lu–Hf: 4286 ± 95 Ma, Sokol et al. 2008; U–Pb: 4350 ± 150 Ma, Terada et al. 2007; $^{207}\text{Pb}/^{206}\text{Pb}$: 4369 ± 7 Ma, Snape et al. 2018). Warren and Taylor (2014) note that Kalahari 009 is an “ancient monomict brecciated Ti-poor basalt ... which is generally interpreted as a mare material (Sokol et al. 2008) despite its position on this diagram...,” a figure such as Fig. 18. Kalahari 009 has lower Ca/Al than do mare basalts, in the direction of material from the feldspathic highlands.

In several other respects, the composition of Kalahari 009 is not like that of any known mare basalt in that it has some FHT characteristics. With 12.8% (Sokol et al. 2008) or 14.9% (Korotev et al. 2009) Al_2O_3 , Kalahari 009 is more aluminous than any mare basalt except the otherwise dissimilar feldspathic basalt of Luna 16 (13.5%). Both Kalahari 009 and its feldspathic pair, Kalahari 008 (585 g; Sokol et al. 2008), are unusual in being rich in Na and poor in Eu, leading to the greatest Na/Eu among lunar meteorites (Fig. S6). Both are also richer in SiO_2 than other lunar meteorites of similar Al_2O_3 concentration (Fig. S31). Most plagioclase in Kalahari 009 is in the An_{88-95} range (Sokol et al. 2008), more calcic than is typical of mare basalt. Finally, Kalahari 009 plots off the Sc–Ti trend of other basalts on Fig. S32. If Kalahari 009 represents a magma, then it is an unusual one, but perhaps one consistent with some style of nonmare volcanism.

The composition of Kalahari 009 can in part be reconciled in terms of more typical mare basalt (but only one with very low abundances of incompatible elements) if it were an impact mixture of ~25% Kalahari 008 and 75% low-Ti basalt with ~20% FeO

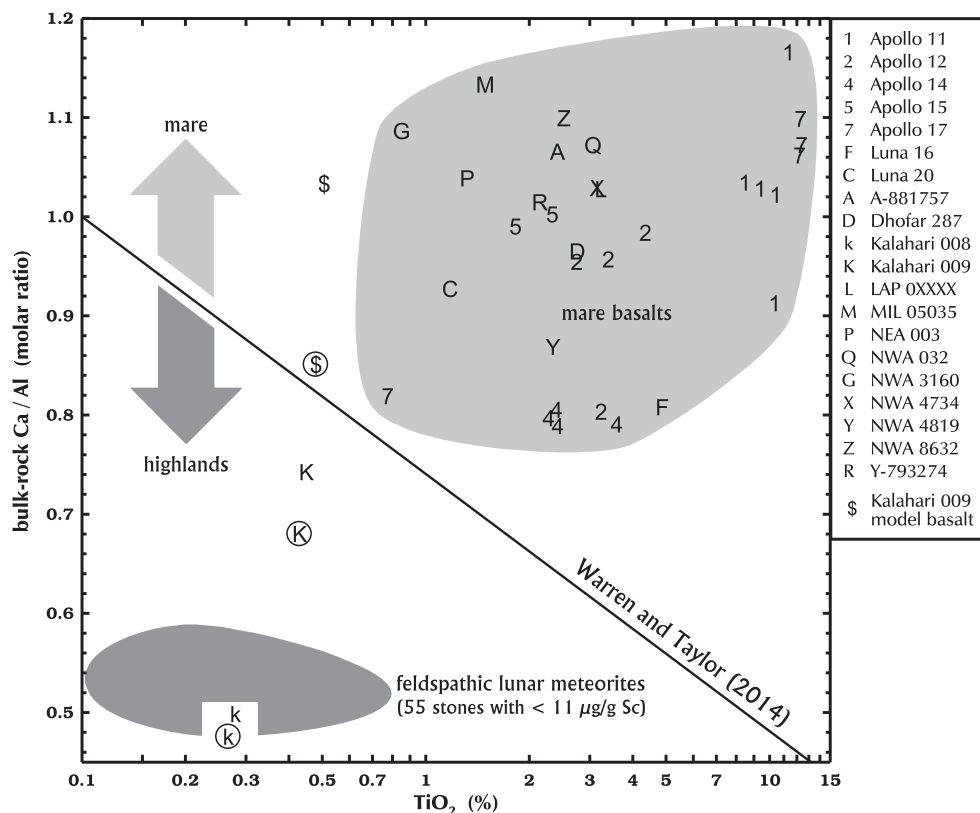


Fig. 18. Comparison of Ca/Al and TiO₂ in meteorites of the feldspathic highlands to mare basalts (after fig. 2 of Warren and Taylor 2014) showing the demarcation between mare and nonmare rocks (diagonal line). The two points each for Kalahari 008 (k) and Kalahari 009 (K) are the data of Sokol et al. (2008, uncircled) and Korotev et al. (2009, circled). Warren and Taylor (2014) note that basaltic breccia Kalahari 009 does not plot with the mare basalts. (The Apollo basalt plotting nearest to Kalahari 009 is the VLT basalt of Apollo 17.) Both Kalahari rocks also have the greatest Na/Eu among lunar meteorites (Fig. S6). The \$ symbols are model-basalt compositions assuming that the K points are mixtures of 75% (\$) and 25% (k); see text. Sources of mare basalt data are given in Fig. S51. TiO₂ values were incorrectly reported in Korotev et al. (2009); correct values are 0.27% for Kalahari 008 and 0.43% for Kalahari 009.

and ~10% Al₂O₃ (“\$” points in Fig. 18; Figs. S64 and S65 in supporting information). The linear distribution of Kalahari 009 points in Fig. S65 is more consistent with a binary mixture than a magma. Concentrations of Ni and Ir in Kalahari 009 are low for melt breccias, however (<150 µg g⁻¹ and < 8 ng g⁻¹), and clasts of feldspathic material are not reported as occurring in Kalahari 009 (Sokol et al. 2008; Snape et al. 2018). Also, the impact mixing scenario drives the Eu concentration of the inferred basalt component to very low concentrations, equivalent only to that of the olivine gabbro in NWA 773 clan (Fig. S64). Thus, the impact-mixture hypothesis is also ambiguous. Kalahari 009 is unique and has an untold story that needs telling.

Although both Sokol et al. (2008) and Snape et al. (2018) note petrographic evidence for terrestrial alteration, Ba concentrations are low and in the range of lunar meteorites from Antarctica for both Kalahari 008 and Kalahari 009 (Fig. 16). K/Th and P/Th are anomalously high, however (Fig. S58).

Miller Range 13317

MIL 13317 (32 g) is a regolith breccia, the fifth lunar meteorite to be found at the Miller Range in Antarctica and the first KREEPy meteorite from Antarctica (10 µg g⁻¹ Sm, Fig. 6). It contains a large variety of lithic clasts including mare basalts, highland fragments, symplectites, norites, and granulites; impact melt breccias; and glass spherules (Shaulis et al. 2016; Zeigler and Korotev 2016; Curran et al. 2019). Compositional trends among subsamples of MIL 13317 and NWA 6687 suggest that both are similar to Apollo 12 soil in that they formed in the PKT primarily from mixtures of mare basalt and KREEP impact melt breccia (Fig. S39).

Lynch 002

Lynch 002 (36.5 g) is the second lunar meteorite recovered in Western Australia (Smith et al. 2012; Robinson et al. 2016). It is compositionally similar to the first, Calalong Creek (19 g), in being moderately

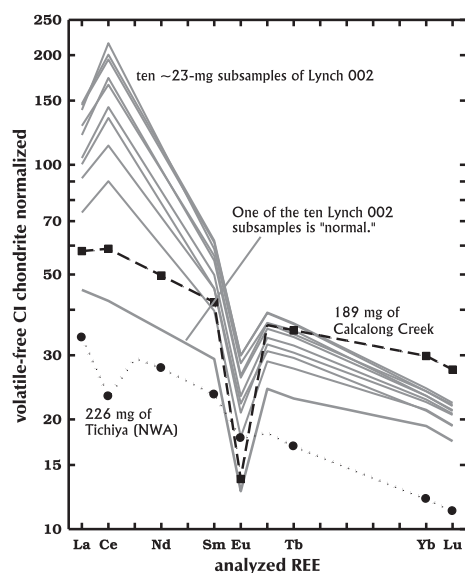


Fig. 19. Nine of the 10 subsamples of Lynch 002 (regolith breccia, Australia) are enriched in light REE compared to, for example, Calalong Creek (regolith breccia, Australia) and have strong positive Ce anomalies ($\text{Ce}/\text{Ce}^* = 1.38\text{--}1.82$). The magnitude of the anomaly (Ce/Ce^*) correlates with La/Sm ($R^2 = 0.84$). One of the subsamples is “normal” ($\text{Ce}/\text{Ce}^* = 1.02$). “The sample (Lynch 002) is moderately to highly weathered” (Smith et al. 2012). Curiously, lunar meteorites with Ce anomalies from northern Africa (e.g., Tichiya) have negative anomalies (Fig. 17).

mafic and moderately rich in incompatible elements. Both are regolith breccias containing clasts of low-Ti or very-low-Ti mare basalt (Hill and Boynton 2003; Smith et al. 2012; Robinson et al. 2016). Pairing is unlikely, however, as they were found 870 km apart and there are some distinct compositional differences (Ir, Cr/Sc; Fig. S66 in supporting information).

Compositionally, the most unusual feature of Lynch 002 is that the bulk composition has been altered by terrestrial weathering processes to an extent greater than that for any other lunar meteorite that we have studied. It is enriched in all REE, but particularly light REE, and has a significant positive Ce anomaly (Fig. 19). The latter feature contrasts with the negative Ce anomalies observed in some NWA meteorites (Fig. 17) and is much more severe than that of the few African lunar meteorites with positive Ce anomalies (Fig. S63). As with the NWA meteorites, the degree of contamination in Lynch 002 is highly variable among our small (22–24 mg) subsamples, with one subsample showing little or no geochemical effects of weathering (“normal” in Fig. 19; Fig. S66). Among the 10 subsamples (Fig. 17), Ce/Ce^* correlates with La/Sm ($R^2 = 0.84$) and the most seriously affected subsample has an La concentration 3× that expected from its Hf concentration (Fig. S66e). La concentrations correlate positively with those of Ba

($R^2 = 0.64$), Sm (0.991), Eu (0.997), Lu (0.88, i.e., heavy REE are also affected), and even Th (0.98) and Co (0.95), but not FeO_T (0.30), Ca (0.21), Na (0.22), Sc (0.21), Hf (0.41), Ta (0.33), U (0.14), Ni (0.00), or Ir (0.03). Br concentrations are the second greatest among hot-desert lunar meteorites, $3.9 \pm 0.9 \mu\text{g g}^{-1}$ (NWA 4485: $6.2 \pm 0.8 \mu\text{g g}^{-1}$). (Lynch 002 was found ~96 km north of the Indian Ocean coast.) Ir and Au are 10.6 ± 1.1 and $4.5 \pm 1.4 \text{ ng g}^{-1}$, typical of lunar regolith breccias.

SUMMARY AND CONCLUSIONS

As of the end of December 2019, 281 lunar meteorite stones totaling 492 kg in mass have been reported from northern Africa. Together, these meteorites constitute, by name, 71% of all known lunar meteorites. Many are paired with others. Among all lunar meteorite stones that have been sufficiently well characterized (86% of the total, mainly by bulk composition but some by unique petrography or find location), we estimate that 131–147 meteoroids and 109–134 launch sites on the Moon are represented.

About a quarter of lunar meteorites of northern Africa are “typical” in being feldspathic (26–32% Al_2O_3 and 3–5% FeO) with low concentrations of incompatible elements (e.g., $0.5\text{--}1.5 \mu\text{g g}^{-1}$ Sm and $0.2\text{--}0.7 \mu\text{g g}^{-1}$ Th). Most such meteorites likely originate from points distant from maria and the Procellarum KREEP Terrane. All feldspathic lunar meteorites are breccias and, mineralogically (Stöffler et al. 1980), nearly all are noritic anorthosites, not anorthosites. There is little evidence among the feldspathic lunar meteorites that highly feldspathic anorthosite (>90% plagioclase), which is ubiquitous at the Apollo 16 landing site, is a common lithology of the FHT (Feldspathic Highlands Terrane).

Among lunar meteorites from northern Africa are several that in detail are unlike rocks in the Apollo collection or lunar meteorites from elsewhere. These include (1) mafic, igneous rocks, most notably the gabbros of NWA 773 and its numerous pairs; (2) moderately mafic, REE-poor, anorthositic troctolite ($\text{Fo}_{77\text{--}79}$) breccias (NWA 5774 and its pairs); (3) two KREEP-rich breccias, one of which (NWA 6687) is like Apollo 12 soil in being a KREEP-mare basalt mixture; and (4) several (~9) meteorites of anorthositic norite mineralogy (7–13% FeO) and low to moderately low concentrations of incompatible elements. Most anorthositic norites are more mafic than typical feldspathic meteorites because they contain clasts of norites, gabbros, gabbro-norites, troctolites, and their more feldspathic equivalents, not mare basalt, because Mg/Fe in these meteorites is greater than any mixture

of typical feldspathic material and mare basalt. Such rocks likely contain mafic, nonmare material from the South Pole–Aitken basin or perhaps the deep crust of the FHT. Nonmare lunar meteorites with high Mg/Fe ($Mg' > 70$) usually contain >10% normative olivine of Fo_{77–79} composition.

In most brecciated lunar meteorites, Ir concentrations are relatively constant and normally distributed among small (20–30 mg) subsamples and equivalent to 0.5–1.7% CM chondrites. Variations among Ir, Au, Ni, and Co concentrations are largely consistent with variations in the relative abundance of an extralunar component of CM or some other chondrite, perhaps largely as micrometeorites (Wasson et al. 1975). Nearly all meteorites in which the mean Ir concentration exceeds 10 ng g^{−1}, however, contain nuggets of FeNi metal with nonchondritic ratios of siderophile elements. Ratios among Ni, Co, and Ir in the metal are more nearly in the range of iron meteorites (e.g., lower Ni/Co than the 20–22 typical of chondrites), however, although not necessarily an exact match to any known groups of iron meteorites.

Nearly all lunar meteorite from northern Africa are contaminated, to varying degrees, with terrestrial Na, Ca, P, K, As, Br, Sr, Sb, Ba, light REE, Au, or U. Ba enrichment, in particular, is characteristic of NWA meteorites, with the NWA 6888 having about 80× the Ba concentration of otherwise similar Apollo rocks. It is, in fact, largely possible to distinguish a lunar meteorite found in northern Africa from one found in Oman on the basis of Sr and Ba concentrations as the latter are characteristically enriched in Sr (Korotev 2012). We document the occurrence of negative Ce anomalies in a few meteorites, with Ce/Ce* as low as 0.66. The anomalies appear to be mainly the result of terrestrial enrichment in light, trivalent REE, although Eu enrichment occurs in some meteorites. We have also observed small positive Ce anomalies in some meteorites.

We provide geochemical evidence that the basalt component of the Kalahari 009 (Botswana) breccia is unlike any known mare basalt and suggest on the basis of its composition and that of its feldspathic pair, Kalahari 008, that Kalahari 009 is a basalt–FHT impact mixture.

Acknowledgments—The authors thank Ryan Zeigler and Axel Wittmann for fused-bead preparation and analysis. Skilled analysts Scott Kuehner (UW) and Paul Carpenter (WUSL) conducted the electron microprobe measurements essential to the petrologic characterization and classification of many of these specimens. We thank Brad Jolliff, Ryan Zeigler, Axel Wittmann, and Julianne Gross for provoking

discussions. We are particularly indebted to Allan Treiman and Paul Warren for insightful reviews. Carl Agee provided samples of specimens classified at the University of New Mexico; other samples were generously donated by L. Atkins, M. Aid, M. Altman, M. Anand, S. Arnold, A. Bevan, A. Bischoff, A. Bouvier, J. Bridges, R. Bartoschewitz, T. Bunch, N. Classen, D. Dickens, S. Decker, M. Farmer, M. Goff, F. Carroll, G. Hupé, J. Haloda, T. Heitz, W. Hsu, A. Jambon, A. Jonikas, K. Keil, A. Love, L. Labenne, M. Morgan, P. Mani, I. Nicklin, M. Ouzillou, D. Ross, S. Ralew, J. Santana, J. Schrader, J. Strope, P. Schmitt-Kopplin, S. Turecki, S. Tutorow, and P. Utas. Adam Hupé provided several grams of clean cutting dust of NWA 5000 for use as an independent standard monitor. This research was funded by NASA grant NNX14AI65G, its predecessor grants, and the McDonnell Center for the Space Sciences.

Editorial Handling—Dr. A. J. Timothy Jull

REFERENCES

- Arai T. and Warren P. H. 1999. Lunar meteorite Queen Alexandra Range 94281: Glass compositions and other evidence for launch pairing with Yamato 793274. *Meteoritics & Planetary Science* 34:209–234.
- Arai T., Takeda H., Yamaguchi A., and Ohtake M. 2008. A new model of lunar crust: Asymmetry in crustal composition and evolution. *Earth, Planets and Space* 60:433–444.
- Arai T., Misawa K., Tomiyama T., Yoshitake M., and Irving A. J. 2009. Constraints on lunar KREEP magmatism: A variety of KREEP basalt derivatives in lunar meteorite NWA 4485 (abstract #2292). 40th Lunar and Planetary Science Conference.
- Arnold J. A., Glotch T. D., Lucey P. G., Song E., Thomas I. R., Bowles N. E., and Greenhagen B. T. 2016. Constraints on olivine-rich rock types on the Moon as observed by Diviner and M3: Implications for the formation of the lunar crust. *Journal of Geophysical Research—Planets* 121:1342–1361.
- Beatty D. W., Hill S. M. R., Albee A. L., Ma M.-S., and Schmitt R. A. 1979. The petrology and chemistry of basaltic fragments from the Apollo 11 soil, part I. Proceedings of the 10th Lunar and Planetary Science Conference. pp. 41–75.
- Bischoff A. and Weber D. 1997. Dar al Gani 262: The first lunar meteorite from the Sahara (abstract). *Meteoritics & Planetary Science* 32:A13–A14.
- Bischoff A., Palme H., Spettel B., Stöffler D., Wänke H., and Ostertag R. 1986. Yamato 82192 and 82193: Two other meteorites of lunar origin (abstract). Papers presented to the Eleventh Symposium on Antarctic Meteorites. pp. 34–36.
- Bischoff A., Weber D., Clayton R. N., Faestermann T., Franchi I. A., Herpers U., Knie K., Korschinek G., Kubik P. W., Mayeda T. K., Merchel S., Michel R., Neumann S., Palme H., Pillinger C. T., Schultz L., Sexton A. S., Spettel B., Verchovsky A. B., Weber H. W., Weckwerth

- G., and Wolf D. 1998. Petrology, chemistry, and isotopic compositions of the lunar highland regolith breccia Dar al Gani 262. *Meteoritics & Planetary Science* 33:1243–1257.
- Borg L. E., Gaffney A. M., Shearer C. K., DePaolo D. J., Hutcheon I. D., Owens T. L., Ramon E., and Brennecka G. 2009. Mechanisms for incompatible-element enrichment on the Moon deduced from the lunar basaltic meteorite Northwest Africa 032. *Geochimica et Cosmochimica Acta* 73:3963–3980.
- Boyle S., Gross J., and Prissel T. C. 2018. Understanding the magnesium-suite lithology and lunar highlands terrain through a detailed investigation of lunar meteorites Northwest Africa (NWA) 10291 and 11182 (abstract #2346). 49th Lunar and Planetary Science Conference.
- Burney D., Neal C. R., Irving A. J., Carpenter P. K., Tepper J. H., and Hoefnagels B. 2020. Petrology and chemical composition of lunar mare diabase Northwest Africa 12839: Comparisons with Apollo basalts (abstract #2613). 51st Lunar and Planetary Science Conference.
- Calzada-Diaz A., Joy K. H., Crawford I. A., and Nordheim T. A. 2015. Constraining the source regions of lunar meteorites using orbital geochemical data. *Meteoritics & Planetary Science* 50:214–228.
- Cao H. J., Ling Z. C., Chen J., and Fu X. H. 2019. Mineralogy and petrography of lunar feldspathic breccia Northwest Africa 11460 (abstract #2359). 50th Lunar and Planetary Science Conference.
- Carpenter P. K., Jolliff B. L., Korotev R. L., Tepper J. H., Irving A. J., and Labenne L. 2019. Petrology and bulk composition of lunar mare basalt breccia Northwest Africa 12384 (abstract #2125). 50th Lunar and Planetary Science Conference.
- Cato M. J., Fagan A. L., and Gross J. 2016. Crystal size distribution of low-Ti lunar basalt-Northwest Africa 8632 (abstract #2751). 47th Lunar and Planetary Science Conference.
- Charlier B., Grove T. L., Namur O., and Holtz F. 2018. Crystallization of the lunar magma ocean and the primordial mantle-crust differentiation of the Moon. *Geochimica et Cosmochimica Acta* 234:50–69.
- Chen J., Jolliff B. L., Korotev R. L., Wang K., Wang A., Carpenter P. K., Chen H., and Ling Z. 2019a. Northwest Africa 10985: A new lunar gabbro? (abstract #2463). 50th Lunar and Planetary Science Conference.
- Chen J., Jolliff B. L., Wang A., Korotev R. L., Wang K., Carpenter P. K., Chen H., Ling Z., Fu X., Ni Y., Cao H., and Huang Y. 2019b. Petrogenesis and shock metamorphism of basaltic lunar meteorites Northwest Africa 4734 and 10597. *Journal of Geophysical Research: Planets* 124:2583–2598.
- Cohen M. E., Kuehner S. M., Tepper J. H., Burney D. C., Neal C. R., Irving A. J., Korotev R. L., and Hoefnagels B. 2019. Mineralogy and bulk composition of lunar mare basalt Northwest Africa 12008 (abstract #2508). 50th Lunar and Planetary Science Conference.
- Collareta A., D'Orazio M., Gemelli M., Pack A., and Folco L. 2016. High crustal diversity preserved in the lunar meteorite Mount DeWitt 12007 (Victoria Land, Antarctica). *Meteoritics & Planetary Science* 51:351–371.
- Corley L. M., McGovern P. J., Kramer G. Y., Lemelin M., Trang D., Gillis-Davis J. J., Taylor G. J., Powell K. E., Kiefer W. S., Wieczorek M., and Zuber M. T. 2018. Olivine-bearing lithologies on the Moon: Constraints on origins and transport mechanisms from M³ spectroscopy, radiative transfer modeling, and GRAIL crustal thickness. *Icarus* 300:287–304.
- Crites S. T. and Lucey P. G. 2015. Revised mineral and Mg# maps of the Moon from integrating results from the Lunar Prospector neutron and gamma-ray spectrometers with Clementine spectroscopy. *American Mineralogist* 100:973–982.
- Cross C. W., Iddings J. P., Pirsson L. V., and Washington H. S. 1902. A quantitative chemico-mineralogical classification and nomenclature of igneous rocks. *Journal of Geology* 10:555–690.
- Crozaz G. and Wadhwa M. 2001. The terrestrial alteration of Saharan Shergottites Dar al Gani 476 and 489: A case study of weathering in a hot desert environment. *Geochimica et Cosmochimica Acta* 65:971–978.
- Crozaz G., Floss C., and Wadhwa M. 2003. Chemical alteration and REE mobilization in meteorites from hot and cold deserts. *Geochimica et Cosmochimica Acta* 67:4727–4741.
- Curran N. C., Joy K. H., Snape J. F., Pernet-Fisher J. F., Gilmour J. D., Nemchin A. A., Whitehouse M. J., and Burgess R. 2019. The early geological history of the Moon inferred from ancient lunar meteorite Miller Range 13317. *Meteoritics & Planetary Science* 54:1401–1430.
- Day J. M. D. and Taylor L. A. 2007. On the structure of mare basalt lava flows from textural analysis of the LaPaz Icefield and Northwest Africa 032 lunar meteorites. *Meteoritics & Planetary Science* 42:3–17.
- Demidova S. I., Nazarov M. A., Anand M., and Taylor L. A. 2003. Lunar regolith breccia Dhofar 287B: A record of lunar volcanism. *Meteoritics & Planetary Science* 38:501–514.
- Demidova S. I., Nazarov M. A., Lorenz C. A., Kurat G., Brandstätter F., and Ntaflos T. 2007. Chemical composition of lunar meteorites and the lunar crust. *Petrology* 15:386–407.
- Dymek R. F., Albee A. L., and Chodos A. A. 1975. Comparative petrology of lunar cumulate rocks of possible primary origin: Dunite 72415, troctolite 76535, norite 78235, and anorthosite 62237. Proceedings, 6th Lunar Science Conference. pp. 301–341.
- Elardo S. M., Shearer Jr. C. K., Fagan A. L., Borg L. E., Gaffney A. M., Burger P. V., Neal C. R., Fernandes V. A., and McCubbin F. M. 2013. The origin of young mare basalts inferred from lunar meteorites Northwest Africa 4734, 032, and LaPaz Icefield 02205. *Meteoritics & Planetary Science* 49:261–291.
- Fagan A. L. and Gross J. 2020. Preliminary melt models of troctolite and anorthosite clasts within Northwest Africa 11303 (abstract #2904). 51st Lunar and Planetary Science Conference.
- Fagan T. J., Taylor G. J., Keil K., Bunch T. E., Wittke J. H., Korotev R. L., Jolliff B. L., Gillis J. J., Haskin L. A., Jarosewich E., Clayton R. N., Mayeda T. K., Fernandes V. A., Burgess R., Turner G., Eugster O., and Lorenzetti S. 2002. Northwest Africa 032: Product of lunar volcanism. *Meteoritics & Planetary Science* 37:371–394.
- Fagan T. J., Taylor J. G., Keil K., Hicks T. L., Killgore M., Bunch T. E., Wittke J. H., Mittlefehldt D. W., Clayton R. N., Mayeda T. K., Eugster O., Lorenzetti S., and Norman M. D. 2003. Northwest Africa 773: Lunar origin and iron-enrichment trend. *Meteoritics & Planetary Science* 38:529–554.
- Fagan A. L., Gross J., Ramsey S., and Turrin B. 2018a. Northwest Africa 8632—Recording young lunar volcanism

- (abstract #2584). 49th Lunar and Planetary Science Conference.
- Fagan A. L., Udry A., Gannon J. P., Cato M. J., and the Spring 2017 WCU Petrology (GEOL 355) class. 2018b. Northwest Africa 8632—Crystal size distribution variation & potential link to Northwest Africa 032 (abstract #2601). 49th Lunar and Planetary Science Conference.
- Fernandes V. A., Burgess R., and Turner G. 2003. ^{40}Ar - ^{39}Ar chronology of lunar meteorites Northwest Africa 032 and 773. *Meteoritics & Planetary Science* 38:555–564.
- Fernandes V. A., Burgess R., and Morris A. 2009. ^{40}Ar - ^{39}Ar age determinations of lunar basalt meteorites Asuka 881757, Yamato 793169, Miller Range 05035, LaPaz Icefield 02205, Northwest Africa 479, and basaltic breccia Elephant Moraine 96008. *Meteoritics & Planetary Science* 44:805–821.
- Fischer-Gödde M., Becker H., and Wombacher F. 2010. Highly siderophile element abundances and $^{187}\text{Os}/^{188}\text{Os}$ in lunar impact melt rocks: Implications for late accretion processes in the Earth-Moon system meteorites (abstract #2262). 41st Lunar and Planetary Science Conference.
- Foley J. A., Coe M. T., Scheffer M., and Wang G. 2003. Regime shifts in the Sahara and Sahel: Interactions between ecological and climatic systems in northern Africa. *Ecosystems* 6:524–539.
- Fukuoka T., Laul J. C., Smith M. R., Hughes S. S., and Schmitt R. A. 1986. Chemistry of Yamato-82192 and -82193 Antarctic meteorites (abstract). Papers presented to the Eleventh Symposium on Antarctic Meteorites. pp. 40–42.
- Gaffney A. M., Borg L. E., DePaolo D. J., and Irving A. J. 2008. Age and isotope systematics of Northwest Africa 4898, a new type of highly depleted mare basalt (abstract #1877). 39th Lunar and Planetary Science Conference.
- Gallant M., Gladman B., and Čuk M. 2009. Current bombardment of the Earth-Moon system: Emphasis on cratering asymmetries. *Icarus* 202:371–382.
- Gillis J. J., Jolliff B. L., and Korotev R. L. 2004. Lunar surface geochemistry: Global concentrations of Th, K, and FeO as derived from lunar prospector and Clementine data. *Geochimica et Cosmochimica Acta* 68:3791–3805. Erratum: *Geochimica et Cosmochimica Acta* 69:5147–5148.
- Gnos E., Hofmann B. A., Al-Kathiri A., Lorenzetti S., Eugster O., Whitehouse M. J., Villa I., Jull A. J. T., Eikenberg J., Spettel B., Krähenbühl U., Franchi I. A., and Greenwood G. C. 2004. Pinpointing the source of a lunar meteorite: Implications for the evolution of the Moon. *Science* 305:657–659.
- Gooley R. C., Brett R., Warner J. L., and Smyth J. R. 1974. A lunar rock of deep crustal origin: Sample 76535. *Geochimica et Cosmochimica Acta* 38:1329–1339.
- Greshake A., Irving A. J., Kuehner S. M., Korotev R. L., Gellissen M., and Palme H. 2008. Northwest Africa 4898: A new high-alumina mare basalt from the Moon (abstract #1631). 39th Lunar and Planetary Science Conference.
- Gross J., Treiman A. H., and Mercer C. M. 2014. Lunar feldspathic meteorites: Constraints on the geology of the lunar highlands, and the origin of the lunar crust. *Earth & Planetary Science Letters* 388:318–328.
- Gross J., Hilton A., Prissel T. C., Setera J. B., Korotev R. L., and Calzada-Diaz A. 2020. Geochemistry and petrogenesis of Northwest Africa (NWA) 10401: A new type of the Mg-suite rocks? *Journal of Geophysical Research: Planets* 125:e2019JE006225.
- Grossman J. N. 2020. Meteoritical Bulletin Database. <https://www.lpi.usra.edu/meteor/>. Accessed January 1, 2020.
- Haloda J., Týcová P., Jakeš P., Gabzdyl P., and Košler J. 2006. Lunar meteorite Northeast Africa 003-B: A new lunar mare basaltic breccia (abstract #2311). 37th Lunar and Planetary Science Conference.
- Haloda J., Týcová P., Korotev R. L., Fernandes V. A., Burgess R., Thöni M., Jelenc M., Jakeš P., Gabzdyl P., and Košler J. 2009. Petrology, geochemistry, and age of low-Ti mare-basalt meteorite Northeast Africa 003-A: A possible member of the Apollo 15 mare basaltic suite. *Geochimica et Cosmochimica Acta* 73:3450–3470.
- Haskin L. A. 1998. The Imbrium impact event and the thorium distribution at the lunar highlands surface. *Journal of Geophysical Research* 103:1679–1689.
- Hilton A., Gross J., Korotev R., and Calzada-Diaz A. 2016. Classifying the unknown—The lunar edition: North West Africa 10401 a new type of the Mg-suite rock? (abstract #1168). 47th Lunar and Planetary Science Conference.
- Hill D. H. and Boynton W. V. 2003. Chemistry of the Calalong Creek lunar meteorite and its relationship to lunar terranes. *Meteoritics & Planetary Science* 38:595–626.
- Hollocher K. T. 2019. Norm Calculation Program. https://minerva.union.edu/hollochk/c_petrology/other_files/norm4.xls. Accessed January 1, 2019.
- Hudgins J. A., Kelley S. P., Korotev R. L., and Spray J. G. 2011a. Mineralogy, geochemistry, and ^{40}Ar – ^{39}Ar geochronology of lunar granulitic breccia Northwest Africa 3163 and paired stones: Comparisons with Apollo samples. *Geochimica et Cosmochimica Acta* 75:2865–2881.
- Hudgins J. A., Spray J. G., and Hawkes C. D. 2011b. Element diffusion rates in lunar granulitic breccias: Evidence for contact metamorphism on the Moon. *American Mineralogist* 96:1673–1685.
- Humayun M. and Irving A. 2008. Impactor metal in gabbroic lunar meteorite Northwest Africa 5000. *Geochimica et Cosmochimica Acta* 72:A402.
- Irving A. J., Kuehner S. M., Korotev R. L., Rumble III D., and Hupé G. M. 2006. Mafic granulitic impactite NWA 3163: A unique meteorite from the deep lunar crust (abstract #1365). 37th Lunar and Planetary Science Conference.
- Irving A. J., Kuehner S. M., Korotev R. L., Rumble III D., and Hupé A. C. 2008. Petrology and bulk composition of large lunar feldspathic leucogabbroic breccia Northwest Africa 5000 (abstract #2186). 39th Lunar and Planetary Science Conference.
- James O. B., Lindstrom M. M., and Flohr M. K. 1989. Ferroan anorthosite from lunar breccia 64435: Implications for the origin and history of lunar ferroan anorthosites. Proceedings, 19th Lunar and Planetary Science Conference. pp. 219–243.
- Johannsen A. 1931. *A descriptive petrography of the igneous rocks*, vol. 1. Chicago: Chicago University Press. 267 pp.
- Jolliff B. L. and Haskin L. A. 1995. Cogenetic rock fragments from a lunar soil: Evidence of a ferroan noritic-anorthosite pluton on the Moon. *Geochimica et Cosmochimica Acta* 59:2345–2374.
- Jolliff B. L., Korotev R. L., and Haskin L. A. 1991. A ferroan region of the lunar highlands as recorded in meteorites MAC88104 and MAC88105. *Geochimica et Cosmochimica Acta* 55:3051–3071.
- Jolliff B. L., Rockow K. M., and Korotev R. L. 1998. Geochemistry and petrology of lunar meteorite Queen

- Alexandra Range 94281, a mixed mare and highland regolith breccia, with special emphasis on very-low-Ti mafic components. *Meteoritics & Planetary Science* 33:581–601.
- Jolliff B. L., Gillis J. J., Haskin L. A., Korotev R. L., and Wieczorek M. A. 2000. Major lunar crustal terranes: Surface expressions and crust-mantle origins. *Journal of Geophysical Research* 105:4197–4416.
- Jolliff B. L., Korotev R. L., Zeigler R. A., Floss C., and Haskin L. A. 2003. Northwest Africa 773: Lunar mare breccia with a shallow-formed olivine-cumulate component, very-low-Ti (VLT) heritage, and a KREEP connection. *Geochimica et Cosmochimica Acta* 67:4857–4879.
- Joy K. H., Crawford I. A., Russell S. S., and Kearsley A. T. 2010. Lunar meteorite regolith breccias: An in situ study of impact melt composition using LA-ICP-MS with implications for the composition of the lunar crust. *Meteoritics & Planetary Science* 45:917–946.
- Joy K. H., Burgess R., Hinton R., Fernandes V. A., Crawford I. A., Kearsley A. T., and Irving A. J. 2011. Petrogenesis and chronology of lunar meteorite Northwest Africa 4472: A KREEPy regolith breccia from the Moon. *Geochimica et Cosmochimica Acta* 75:2420–2452.
- Kagi H. and Takahashi K. 2008. Relationship between positive Ce anomaly and adsorbed water in Antarctic lunar meteorites. *Meteoritics & Planetary Science* 33:1033–1040.
- Kent J. J., Brandon A. D., Joy K. H., Peslier A. H., Lapen T. J., Irving A. J., and Coleff D. M. 2017. Mineralogy and petrogenesis of lunar magnesian granulitic meteorite Northwest Africa 5744. *Meteoritics & Planetary Science* 52:1916–1940.
- Koeberl C. 1988. Trace element geochemistry of lunar meteorites Yamato-791197 and -82192. *Proceedings of the NIPR Symposium on Antarctic Meteorites* 1:122–134.
- Koeberl C., Warren P. H., Lindstrom M. M., Spettel B., and Fukuoka T. 1989. Preliminary examination of the Yamato-86032 lunar meteorite: II. Major and trace element chemistry. *Proceedings of the NIPR Symposium on Antarctic Meteorites* 2:15–24.
- Korotev R. L. 1987. The meteoritic component of Apollo 16 noritic impact melt breccias. *Journal of Geophysical Research* 92:E491–E512.
- Korotev R. L. 1997. Some things we can infer about the Moon from the composition of the Apollo 16 regolith. *Meteoritics & Planetary Science* 32:447–478.
- Korotev R. L. 2000. The great lunar hot spot and the composition and origin of the Apollo mafic (“LKFM”) impact-melt breccias. *Journal of Geophysical Research* 105:4317–4345.
- Korotev R. L. 2005. Lunar geochemistry as told by lunar meteorites. *Chemie der Erde* 65:297–346.
- Korotev R. L. 2012. Lunar meteorites from Oman. *Meteoritics & Planetary Science* 47:1365–1402.
- Korotev R. L. 2013. Composition of Lynch 002 lunar meteorite (abstract #5021). 76th Annual Meeting of the Meteoritical Society. *Meteoritics & Planetary Science* 48 (Supp.).
- Korotev R. L. 2017. Update (2012–2017) on lunar meteorites from Oman. *Meteoritics & Planetary Science* 52:1251–1256.
- Korotev R. L. and Zeigler R. A. 2014. ANSMET meteorites from the Moon. In *35 seasons of U.S. Antarctic meteorites*, edited by Righter K., Corrigan C. M., McCoy T. J., and Harvey R. Washington, D.C.: American Geophysical Union. pp. 101–130.
- Korotev R. L., Jolliff B. L., Zeigler R. A., Gillis J. J., and Haskin L. A. 2003. Feldspathic lunar meteorites and their implications for compositional remote sensing of the lunar surface and the composition of the lunar crust. *Geochimica et Cosmochimica Acta* 67:4895–4923.
- Korotev R. L., Irving A. J., and Bunch T. E. 2008. Keeping up with the lunar meteorites—2008 (abstract #1209). 39th Lunar and Planetary Science.
- Korotev R. L., Zeigler R. A., Jolliff B. L., Irving A. J., and Bunch T. E. 2009. Compositional and lithological diversity among brecciated lunar meteorites of intermediate iron composition. *Meteoritics & Planetary Science* 44:1287–1322.
- Korotev R. L., Jolliff B. L., and Zeigler R. A. 2010. On the origin of the Moon’s feldspathic highlands, pure anorthosite, and the feldspathic lunar meteorites (abstract #1440). 41st Lunar and Planetary Science Conference.
- Korotev R. L., Jolliff B. L., Zeigler R. A., Seddio S. M., and Haskin L. A. 2011. Apollo 12 revisited. *Geochimica et Cosmochimica Acta* 75:1540–1573.
- Korotev R. L., Irving A. J., Wittmann A., Kuehner S. M., Chennaoui-Aoudjehane H., and Labenne L. 2015. Petrology and composition of lunar mare basalt meteorite Northwest Africa 8632 from Chwichiya, Morocco (abstract #1195). 46th Lunar and Planetary Science Conference.
- Kuehner S. M., Irving A. J., Rumble III D., Hupé A. C., and Hupé G. M. 2005. Mineralogy and petrology of lunar meteorite NWA 3136: A glass-welded mare regolith breccia of mixed heritage (abstract #1228). 36th Lunar and Planetary Science Conference.
- Kuehner S. M., Irving A. J., Gellissen M., and Korotev R. L. 2010. Petrology and composition of lunar troctolitic granulite Northwest Africa 5744: A unique recrystallized, magnesian crustal sample (abstract #1552). 41st Lunar and Planetary Science Conference.
- Lawrence D. J., Feldman W. C., Barraclough B. L., Binder A. B., Elphic R. C., Maurice S., Miller M. C., and Prettyman T. H. 2000. Thorium abundances on the lunar surface. *Journal of Geophysical Research* 105:20,307–20,331.
- Le Feuvre M. and Wieczorek M. A. 2008. Non-uniform cratering of the terrestrial planets. *Icarus* 197:291–306.
- Lemelin M., Lucey P. G., Miljković K., Gaddis L. R., Hare T., and Ohtake M. 2019. The compositions of the lunar crust and upper mantle: Spectral analysis of the inner rings of lunar impact basins. *Planetary and Space Science* 165:30–243.
- Li S., Hsu W., Guan Y., Wang L., and Wang Y. 2016. Petrogenesis of the Northwest Africa 4898 high-Al mare basalt. *Meteoritics & Planetary Science* 51:1268–1288.
- Lindstrom M. M. and Lindstrom D. J. 1986. Lunar granulites and their precursor anorthositic norites of the early lunar crust. *Journal of Geophysical Research* Supplement 91: D263–D276.
- Lindstrom M. M., Knapp S. A., Shervais J. W., and Taylor L. A. 1984. Magnesian anorthosites and associated troctolites and dunite in Apollo 14 breccias. *Journal of Geophysical Research* Supplement 89:C41–C62.
- Lindstrom M. M., Lindstrom D. J., Korotev R. L., and Haskin L. A. 1986. Lunar meteorite Yamato-791197: A polymict anorthositic norite from the lunar highlands.

- Memoirs of the National Institute of Polar Research, Special Issue* 41:58–75.
- Lodders K. and Fegley B. Jr. 1998. *The planetary scientist's companion*. New York: Oxford University Press. 371 pp.
- Longhi J. 2003. A new view of lunar ferroan anorthosites: Postmagma ocean petrogenesis. *Journal of Geophysical Research—Planets* 108:2-1–2-16.
- Lucey P. G., Korotev R. L., Gillis J. J., Taylor L. A., Lawrence D., Campbell B. A., Elphic R., Feldman B., Hood L. L., Hunten D., Mendillo M., Noble S., Papike J. J., Reedy R. C., Lawson S., Prettyman T., Gasnault O., and Maurice S. 2006. Understanding the lunar surface and space-moon interactions. In *New views of the Moon*, edited by Jolliff B. L., Wieczorek M. A., Shearer C. K., and Neal C. R. Reviews in Mineralogy & Geochemistry, vol. 60. Chantilly, Virginia: Mineralogical Society of America. pp. 83–219.
- Lonning N. G. and Gross J. 2019. Lunar feldspathic regolith breccia with magnesium-rich components. Northwest Africa 11303 (abstract #2047). 50th Lunar and Planetary Science Conference.
- McLeod C. L., Brandon A. D., Fernandes V. A., Peslier A. H., Fritz J., Lapen T. J., Shafer J. T., Butcher A. R., and Irving A. J. 2016. Constraints on formation and evolution of the lunar crust from feldspathic granulitic breccias NWA 3163 and 4881. *Geochimica et Cosmochimica Acta* 187:350–374.
- Mercer C. N., Treiman A. H., and Joy K. H. 2013. New lunar meteorite Northwest Africa 2996: A window into farside lithologies and petrogenesis. *Meteoritics & Planetary Science* 48:289–315.
- Mészáros M., Hofmann B. A., Lanari P., Korotev R. L., Gnos E., Greber N. D., Leya I., Greenwood R. C., Jull A. J. T., Al-Wagdani K., Mahjoub A., Al-Solami A. A., and Habibullah S. N. 2016. Petrology and geochemistry of feldspathic impact-melt breccia Abar al' Uj 012, the first lunar meteorite from Saudi Arabia. *Meteoritics & Planetary Science* 51:1830–1848.
- Morota T., Ukai T., and Furumoto M. 2005. Influence of the asymmetrical cratering rate on the lunar cratering chronology. *Icarus* 173:322–324.
- Nagaoka H., Karouji Y., and Takeda H. 2015. Mineralogy and petrology of lunar meteorite Northwest Africa 2977 consisting of olivine cumulate gabbro including inverted pigeonite. *Earth, Planets and Space* 67:200. <https://doi.org/10.1186/s40623-015-0368-y>
- Nagurny A. B., Treiman A. H., and Spudis P. D. 2016. Petrology, bulk composition, and provenance of meteorite Northwest Africa 5000 (abstract #1103). 46th Lunar and Planetary Science Conference.
- Nishiizumi K. 2003. Exposure histories of lunar meteorites (abstract #56). Papers presented to the International Symposium: Evolution of Solar System Materials: A New Perspective from Antarctic Meteorites.
- Nishiizumi K. and Caffee M. W. 2013. Relationships among six lunar meteorites from Miller Range, Antarctica based on cosmogenic radionuclides (abstract #2715). 44th Lunar and Planetary Science Conference.
- Nishiizumi K., Caffee M. W., and Jull A. J. T. 2016. Exposure history of Mount DeWitt 12007 and proposed launch-paired Northwest Africa 4884, 7611, and 8277 lunar meteorites (abstract #6514). 79th Annual Meeting of the Meteoritical Society.
- North-Valencia S. N., Jolliff B. L., and Korotev R. L. 2014. Ferroan gabbro and leucogabbro lithologies in NWA 3170, possible petrogenetic link and comparison to NWA 2727 (abstract #2858). 45th Lunar and Planetary Science Conference.
- Nyquist L., Bogard D., Yamaguchi A., Shih C.-Y., Karouji Y., Ebihara M., Reese Y., Garrison D., McKay G., and Takeda H. 2006. Feldspathic clasts in Yamato-86032: Remnants of the lunar crust with implications for its formation and impact history. *Geochimica et Cosmochimica Acta* 70:5990–6015.
- O'Donnell S. P., Jolliff B. L., Zeigler R. A., and Korotev R. L. 2008. Identifying the mafic components in lunar regolith breccia NWA 3136 (abstract #2507). 39th Lunar and Planetary Science Conference.
- Ohtake M., Takeda H., Matsunaga T., Yokota Y., Haruyama J., Morota T., Yamamoto S., Ogawa Y., Hiroi T., Karouji Y., Saiki K., and Lucey P. G. 2012. Asymmetric crustal growth on the Moon indicated by primitive farside highland materials. *Nature Geoscience* 5:384–388.
- Ostertag R., Stöffler D., Bischoff A., Palme H., Schultz L., Spettel B., Weber H., Weckwerth G., and Wänke H. 1986. Lunar meteorite Yamato-791197: Petrography, shock history and chemical composition. *Memoirs of the National Institute of Polar Research, Special Issue* 41:17–44.
- Palme H., Spettel B., Jochum K. P., Dreibus G., Weber H., Weckwerth G., Wänke H., Bischoff A., and Stöffler D. 1991. Lunar highland meteorites and the composition of the lunar crust. *Geochimica et Cosmochimica Acta* 55:3105–3122.
- Pernet-Fisher J. F., Deloule E., and Joy K. H. 2019. Evidence of chemical heterogeneity within lunar anorthosite parental magmas. *Geochimica et Cosmochimica Acta* 266:109–130.
- Prettyman T. H., Hagerty J. J., Elphic R. C., Feldman W. C., Lawrence D. J., McKinney G. W., and Vaniman D. T. 2006. Elemental composition of the lunar surface: analysis of gamma ray spectroscopy data from Lunar Prospector. *Journal of Geophysical Research—Planets* 111:E12007.
- Puchtel I. S., Walker R. J., James O. B., and Kring D. A. 2008. Osmium isotope and highly siderophile element systematics of lunar impact melt breccias: Implications for the late accretion history of the Moon and Earth. *Geochimica et Cosmochimica Acta* 72:3022–3042.
- Qin L., Day J. M. D., and Tait K. T. 2020. Oxidative impact processes revealed in Northwest Africa 11223 (abstract #2318). 51st Lunar and Planetary Science Conference.
- Raedeke L. D. and McCallum I. S. 1980. A comparison of fractionation trends in the lunar crust and the Stillwater Complex. New York: Pergamon Press. pp. 133–153.
- Roberts S. E., McCanta M. C., Jean M. M., and Taylor L. A. 2019. New lunar meteorite NWA 10986: A mingled impact melt breccia from the highlands—A complete cross section of the lunar crust. *Meteoritics & Planetary Science* 54:3018–3035.
- Robinson K. L. and Kring D. A. 2018. The Northwest Africa 5744 group: A glimpse into Schrödinger-like lithologies? (abstract #1635). 49th Lunar and Planetary Science Conference.
- Robinson K. L., Smith C. L., Kearsley A. T., Bevan A. W. R., and Anand M. 2016. The Lynch 002 lunar meteorite revisited (abstract #1470). 46th Lunar and Planetary Science Conference.
- Russell S. S., Joy K. H., Jeffries T. E., Consolmagno G. J., and Kearsley A. 2014. Heterogeneity in lunar anorthosite meteorites: Implications for the lunar magma ocean model. *Philosophical Transactions of the Royal Society A* 372:20130241.

- Shaulis B. J., Kring D. A., Lapen T. J., and Righter M. 2016. Petrology and distribution of U-Pb ages in lunar meteorite breccia Miller Range (MIL) 13317 (abstract #2027). 47th Lunar and Planetary Science Conference.
- Shaulis B. J., Righter M., Lapen T. J., Jolliff B. J., and Irving A. J. 2017. 3.1 Ga crystallization age for magnesian and ferroan gabbro lithologies in the Northwest Africa 773 clan of lunar meteorites. *Geochimica et Cosmochimica Acta* 213:435–456.
- Shi E., Carpenter P. K., Jolliff B. L., Chen J., Wang A., Tepper J. H., Irving A. J., Burney D. C., and Neal C. R. 2020. Mineralogical and petrological analysis of lunar mare gabbro meteorite Swayyah 001 (abstract #2923). 50th Lunar and Planetary Science Conference.
- Smith C. L., Kearsley A. T., Birmingham K. R., Deacon G. L., Kurahashi E., Franchi I. A., and Bevan A. W. R. 2012. Lynch 002: A new lunar meteorite from the Nullarbor Desert, Western Australia (abstract #5137). 75th Annual Meeting of the Meteoritical Society.
- Snape J. F., Curran N. M., Whitehouse M. J., Nemchin A. A., Joy K. H., Hopkinson T., Anand M., Bellucci J. J., and Kenny G. G. 2018. Ancient volcanism on the Moon: Insights from Pb isotopes in the MIL 13317 and Kalahari 009 lunar meteorites. *Earth and Planetary Science Letters* 502:84–95.
- Sokol A. K., Fernandes V. A., Schulz T., Bischoff A., Burgess R., Clayton R. N., Münker C., Nishiizumi K., Palme H., Schultz L., Weckwerth G., Mezger K., and Horstmann M. 2008. Geochemistry, petrology and ages of the lunar meteorites Kalahari 008 and 009: New constraints on early lunar evolution. *Geochimica et Cosmochimica Acta* 72:4845–4873.
- Stephant A., Anand M., Ashcroft H. O., Zhao X., Hu S., Korotev R. L., Strekopytov S., Greenwood R. C., Humphreys-Williams E., Liu Y., Tang G., Li Q., and Franchi I. A. 2019. An ancient reservoir of volatiles in the Moon sampled by lunar meteorite Northwest Africa 10989. *Geochimica et Cosmochimica Acta* 266:163–183.
- Stöffler D., Knöll H.-D., Marvin U. B., Simonds C. H., and Warren P. H. 1980. Recommended classification and nomenclature of lunar highlands rocks—A committee report. New York: Pergamon Press. pp. 51–70.
- Takeda H., Yamaguchi A., Bogard D. D., Karouji Y., Ebihara M., Ohtake M., Saiki K., and Arai T. 2006. Magnesian anorthosites and a deep crustal rock from the farside crust of the Moon. *Earth and Planetary Science Letters* 247:171–184.
- Tang C. P., Sawchuk K., and Warren P. H. 2018. A textural/mineralogical gradient within vitrophyric mare basalt Northwest Africa (NWA) 8632 (abstract #2029). 49th Lunar and Planetary Science Conference.
- Terada K., Anand M., Sokol A. K., Bischoff A., and Sano Y. 2007. Cryptomare magmatism 4.35 Gyr ago recorded in lunar meteorite Kalahari 009. *Nature* 450:849–853.
- Treiman A. H. and Coleff D. M. 2018. Lunar meteorite Northwest Africa (NWA) 11421: X-ray tomography and preliminary petrology (abstract #6329). 81st Annual Meeting of the Meteoritical Society.
- Treiman A. H. and Semprich J. 2019. Dunite in lunar meteorite Northwest Africa 11421: Petrology and origin (abstract #1225). 50th Lunar and Planetary Science Conference.
- Treiman A. H., Maloy A. K., Shearer C. K. Jr., and Gross J. 2010. Magnesian anorthositic granulites in lunar meteorites Allan Hills A81005 and Dhofar 309: Geochemistry and global significance. *Meteoritics & Planetary Science* 45:163–180.
- Valencia S. N., Jolliff B. L., and Korotev R. L. 2019. Petrography, relationships, and petrogenesis of the gabbroic lithologies in Northwest Africa 773 clan members Northwest Africa 773, 2727, 3160, 3170, 7007, and 10656. *Meteoritics & Planetary Science* 54:2083–2115.
- Vaniman D., Dietrich J., Taylor G. J., and Heiken G. 1991. Exploration, samples, and recent concepts of the Moon. In *Lunar sourcebook*, edited by Heiken G. H., Vaniman D. T., and French B. M. Cambridge: Cambridge University Press. pp. 6–26.
- Warren P. H. 1986a. Anorthosite assimilation and the origin of the Mg/Fe-related bimodality of pristine Moon rocks: Support for the magmasphere hypothesis. *Journal of Geophysical Research* 91:D331–D343.
- Warren P. H. 1986b. The bulk-Moon MgO/FeO ratio: A highlands perspective. In *Origin of the Moon*, edited by Hartmann W. K., Phillips R. J., and Taylor G. J. Houston, Texas: Lunar and Planetary Institute. pp. 279–310.
- Warren P. H. 1990. Lunar anorthosites and the magma-ocean plagioclase-flotation hypothesis: Importance of FeO enrichment in the parent magma. *American Mineralogist* 75:46–58.
- Warren P. H. 1993. A concise compilation of petrologic information on possibly pristine nonmare Moon rocks. *American Mineralogist* 78:360–376.
- Warren P. H. and Kallemeyn G. W. 1986. Geochemistry of lunar meteorite Yamato-791197: Comparison with ALHA81005 and other lunar samples. *Memoirs of the National Institute of Polar Research, Special Issue* 41:3–16.
- Warren P. H. and Kallemeyn G. W. 1991. Geochemical investigations of five lunar meteorites: Implications for the composition, origin and evolution of the lunar crust. *Proceedings of the NIPR Symposium on Antarctic Meteorites* 4:91–117.
- Warren P. H. and Taylor G. J. 2014. The Moon. In *Planets, asteroids, comets and the solar system*, edited by Davis A. M., Treatise on Geochemistry, 2nd ed. New York: Elsevier. pp. 213–250.
- Warren P. H. and Wasson J. T. 1977. Pristine nonmare rocks and the nature of the lunar crust. Proceedings, 8th Lunar Planetary Science Conference. pp. 2215–2235.
- Warren P. H. and Wasson J. T. 1980. Further foraging for pristine nonmare rocks: Correlations between geochemistry and longitude. Proceedings, 11th Planetary Science Conference. pp. 431–470.
- Warren P. H., Jerde E. A., and Kallemeyn G. W. 1989. Lunar meteorites: Siderophile element contents, and implications for the composition and origin of the Moon. *Earth and Planetary Science Letters* 91:245–260.
- Warren P. H., Ulff-Møller F., and Kallemeyn G. W. 2005. “New” lunar meteorites: Impact melt and regolith breccias and large-scale heterogeneities of the upper lunar crust. *Meteoritics & Planetary Science* 40:989–1014.
- Wasson J. T. 2019. Campo del Cielo: A Campo by any other name. *Meteoritics & Planetary Science* 54:280–289.
- Wasson J. T., Boynton W. V., Chou C.-L., and Baedeker P. A. 1975. Compositional evidence regarding the influx of interplanetary materials onto the lunar surface. *The Moon* 13:121–141.
- Webb S., Neal C. R., Gawronska A., and Day J. M. D. 2019. Crystal size distribution patterns for lunar meteorites Northwest Africa 12008, 4898, 8632, 3136 and three

- LaPaz Icefield lunar meteorites (abstract #2686). 50th Lunar and Planetary Science Conference.
- Welch B. L. 1947. The generalization of “Student’s” problem when several different population variances are involved. *Biometrika* 34:28–35.
- Wieczorek M. A., Jolliff B. L., Khan A., Pritchard M. E., Weiss B. P., Williams J. G., Hood L. L., Righter K., Neal C. R., Shearer C. K., McCallum I. S., Tompkins S., Hawke B. R., Patterson C., Gillis J. J., and Bussey B. 2006. The constitution and structure of the lunar interior. In *New views of the Moon*, edited by Jolliff B. L., Wieczorek M. A., Shearer C. K., and Neal C. R. Reviews in Mineralogy and Geochemistry, vol. 60. Washington, D.C.: Mineralogical Society of America. pp. 221–364.
- Will P., Busemann H., Riebe M. E. I., and Maden C. 2019. Regolith history of six lunar regolith breccias derived from noble gas elemental and isotopic abundances (abstract #6494). 82nd Annual Meeting of the Meteoritical Society.
- Xu X., Hui H., Chen W., Huang S., Neal C. R., and Xu X. 2020. Formation of lunar highlands anorthosites. *Earth and Planetary Science Letters* 36:116138.
- Yamaguchi A., Karouji Y., Takeda H., Nyquist L., Bogard D., Ebihara M., Shih C. Y., Reese Y., Garrison D., Park J., and McKay G. 2010. The variety of lithologies in the Yamato-86032 lunar meteorite: Implications for formation processes of the lunar crust. *Geochimica et Cosmochimica Acta* 74:4507–4530.
- Yamamoto S., Nakamura R., Matsunaga T., Ogawa Y., Ishihara Y., Morota T., Hirata N., Ohtake M., Hiroi T., Yokota Y., and Haruyama J. 2010. Possible mantle origin of olivine around lunar impact basins detected by SELENE. *Nature Geoscience* 3:533–536.
- Yanai K. and Kojima H. 1984. Lunar meteorites in Japanese collection of the Yamato meteorites (abstract). *Meteoritics* 19:342.
- Zeigler R. A. and Korotev R. L. 2016. Petrography and geochemistry of lunar meteorite Miller Range 13317 (abstract #2554). 47th Lunar and Planetary Science Conference.
- Zeigler R. A., Korotev R. L., Jolliff B. L., and Haskin L. A. 2005. Petrology and geochemistry of the LaPaz Icefield basaltic lunar meteorite and source-crater pairing with Northwest Africa 032. *Meteoritics & Planetary Science* 40:1073–1102.
- Zeigler R. A., Korotev R. L., and Jolliff B. L. 2007. Petrography, geochemistry, and pairing relationships of basaltic lunar meteorite stones NWA 773, NWA 2700, NWA 2727, NWA 2977, and NWA 3160 (abstract #2109). 38th Lunar and Planetary Science Conference.
- Zeng X., Joy K. H., Li S., Pernet-Fisher J., Li X., Martin D. J. P., Li Y., and Wang S. 2019. Multiple lithic clasts in lunar breccia Northwest Africa 7948 and implication for the lithologic components of lunar crust. *Meteoritics & Planetary Science* 53:1030–1050.
- Zipfel J., Spettel B., Palme H., Wolf D., Franchi I., Sexton A. S., Pillinger C. T., and Bischoff A. 1998. Dar al Gani 400: Chemistry and petrology of the largest lunar meteorite. *Meteoritics & Planetary Science* 33:A171.

SUPPORTING INFORMATION

Additional supporting information may be found in the online version of this article.

Data S1. Table of contents.